Designing localized electromagnetic fields in a source-free space

George N. Borzdov
Department of Theoretical Physics, Belarusian State University, Minsk, Belarus
(Received 20 February 2002; published 21 June 2002)

An approach to characterizing and designing localized electromagnetic fields, based on the use of differentiable manifolds, differentiable mappings, and the group of rotation, is presented. By way of illustration, novel families of exact time-harmonic solutions to Maxwell's equations in the source-free space—localized fields defined by the rotation group—are obtained. The proposed approach provides a broad spectrum of tools to design localized fields, i.e., to build-in symmetry properties of oscillating electric and magnetic fields, to govern the distributions of their energy densities (both size and form of localization domains), and to set the structure of time-average energy fluxes. It is shown that localized fields can be combined as constructive elements to obtain a complex field structure with desirable properties, such as one-, two-, or three-dimensional field gratings. The proposed approach can be used in designing localized electromagnetic fields to govern motion and state of charged and neutral particles. As an example, motion of relativistic electrons in one-dimensional and three-dimensional field gratings is treated.

DOI: 10.1103/PhysRevE.65.066612 PACS number(s): 03.50.De, 34.90.+q, 41.20.Jb, 41.75.−i

I. INTRODUCTION

In the last two decades, the problem of localized transmission of electromagnetic and acoustic energy has been much investigated (see, for example, Refs. [1–21] and references therein). Many so-called localized wave solutions to the homogeneous scalar wave equation and Maxwell's equations, that describe localized, slowly decaying transmission of energy, have been found. They include focus wave modes [1,2], modulated, moving Gaussian pulses [3], electromagnetic missiles [4], Bessel and Bessel-Gauss beams [5,6], acoustic [7] and electromagnetic [8,9] directed-energy pulse trains (ADEPT's and EDEPT's), moving modified Bessel-Gauss pulses [13], moving pulses with Gaussian localization in both longitudinal and transverse directions [21], etc. It was shown [8,9,16] that localized fields can be realized physically, they can be excited from finite apertures. To this end, Ziolkowski suggested to use an array that has independently addressable elements [12]. The existence of ADEPT's was confirmed by Ziolkowski *et al.* with experiments using ultrasound in water [7,10]. Recently, Saari and Reivelt proposed an approach to constructing realizable schemes for generation of localized fields in optic region [19,20]. It was shown that they can be used to generate good approximation to focus wave modes.

Plane-wave expansions play a very important role in the analysis of localized fields. By using the Fourier transform, a method for obtaining separable and nonseparable localized solutions of constant coefficient homogeneous partial differential equations was developed by Donnelly and Ziolkowski [14,15]. It was shown by Shaarawi *et al.* that the source-free focus wave modes are composed of backward and forward propagating homogeneous plane waves [17].

By using expansions in plane waves, we have introduced [22,23] a specific type of linear fields—beams defined by a set of orthonormal scalar functions on a two-dimensional or three-dimensional manifold (beam manifold). The proposed approach enables one to obtain a set of orthonormal beams and various families of localized fields: three-dimensional standing waves, moving and evolving whirls. This can be applied to any linear field, such as electromagnetic waves in free space, isotropic, anisotropic, and bianisotropic media [22–26], elastic waves in isotropic and anisotropic media [27,28], sound waves [27], weak gravitational waves [24], etc. By way of illustration, we have treated [22–28] the fields defined by the spherical harmonics. In particular, we have presented [26] an approach to characterizing electromagnetic fields and complex media, based on the use of novel families of electromagnetic beams. It was shown [28] that the localized elastic fields [27] can be combined into a complex field structure, such as an ultrasonic diffraction grating. This makes them promising tools to control laser radiation.

In this paper, we propose a different technique for obtaining localized exact solutions of Maxwell's equations. It has extended potentialities for field design. To illustrate this, we present unique families of localized fields in free space and some examples of combining them into a complex field structure. The proposed approach can be used in designing localized electromagnetic fields to govern motion and state of charged and neutral particles. We illustrate this on an example of relativistic electrons moving in the designed field gratings.

The plan of the paper is as follows. In Sec. II, we present an approach to characterizing and designing localized electromagnetic fields, based on the use of differentiable manifolds and differentiable mappings. In Sec. III, we introduce a family of localized fields defined by the group of rotation. Localized electromagnetic fields with spherical and toroidal beam manifolds are presented in Secs. IV and V, respectively. In Sec. VI, two examples of combining localized fields into a complex field structure are presented. Motion of relativistic electrons in one-dimensional and three-dimensional field gratings is also treated in this section. Concluding remarks are made in Sec. VII.

II. PARAMETRIZATION OF PLANE-WAVE SUPERPOSITIONS

In this paper, we use both four-dimensional and three-dimensional electromagnetic field equations. The four-dimensional formalism makes it possible to construct various exact covariant solutions of plane waves parametrized by some geometrical objects independent of the reference frame. The three-dimensional formalism is convenient for description of some special fields, such as time harmonic or quasimonochromatic fields in some given reference frame.

A. Lorentz covariant parametrization

1. Eigenwaves

Using the intrinsic tensor technique [29,30], the four–dimensional electromagnetic field tensor F can be written as

$$F=\mathbf{B}\rfloor*\vartheta^4+E\wedge\vartheta^4=\sum_{1\leqslant i<j\leqslant 4}F_{ij}\vartheta^i\wedge\vartheta^j=B_3\vartheta^1\wedge\vartheta^2-B_2\vartheta^1\wedge\vartheta^3+B_1\vartheta^2\wedge\vartheta^3+(E_1\vartheta^1+E_2\vartheta^2+E_3\vartheta^3)\wedge\vartheta^4, \tag{1}$$

where

$$E=-\mathbf{e}_4\rfloor F=\sum_{i=1}^{3}E_i\vartheta^i, \tag{2a}$$

$$\mathbf{B}=*\mathbf{e}_4\lfloor F=\sum_{i=1}^{3}B^i\mathbf{e}_i, \tag{2b}$$

$E_i=E^i$, $B_i=B^i$, and $i=1,2,3$. Here, $(\mathbf{e}_i)$ and (ϑ^i) are the dual orthonormal bases in the Minkowski vector space V and its dual V^* (the space of one-forms or, in other words, the space of covariant vectors); $\otimes$, $\wedge$, $\rfloor$, and $\lfloor$ are the tensor, exterior, and interior products; $*$ is the star operator. In this paper, we distinguish the r-vectors (antisymmetric r contravariant tensors) from other tensors by the bold type, in particular, $\mathbf{B}\in V$ and $E\in V^*$. The covariant and contravariant metric tensors have the form

$$g=\vartheta^1\otimes\vartheta^1+\vartheta^2\otimes\vartheta^2+\vartheta^3\otimes\vartheta^3-\vartheta^4\otimes\vartheta^4, \tag{3a}$$

$$g^{-1}=\mathbf{e}_1\otimes\mathbf{e}_1+\mathbf{e}_2\otimes\mathbf{e}_2+\mathbf{e}_3\otimes\mathbf{e}_3-\mathbf{e}_4\otimes\mathbf{e}_4, \tag{3b}$$

respectively. To simplify the subsequent relations, we use the Gaussian units.

Electromagnetic homogeneous plane waves (eigenwaves), propagating in the source-free space, can be written as

$$F(\mathbf{x})=F(\mathbf{r},t)=F(0)e^{i\Phi}, \tag{4}$$

where

$$\Phi=\mathbf{x}\cdot\mathbf{K}=\mathbf{k}\cdot\mathbf{r}-\omega t, \tag{5}$$

$\mathbf{x}=\mathbf{r}+ct\mathbf{e}_4$ is the four-dimensional position vector, and $\mathbf{K}=\mathbf{k}+\mathbf{e}_4\omega/c=k(\hat{\mathbf{k}}+\mathbf{e}_4)$ is the four-dimensional wave vector. Here, t and $\mathbf{r}$ are the time and the three-dimensional radius vector in a Lorentz frame L with the basis $(\mathbf{e}_i)$, ω and $\mathbf{k}$ are the angular frequency and the three-dimensional wave vector in this frame, c is the velocity of light in vacuum, $\hat{\mathbf{k}}=\mathbf{k}/k$ is the unit wave normal, $k=\omega/c=2\pi/\lambda$ is the wave number, and λ is the wavelength.

2. Beam manifold $\mathcal{B}$

To compose an electromagnetic field of eigenwaves propagating in the source-free space, one must specify their propagation directions, frequencies or wave numbers, polarizations, intensities, and initial phases. Since the eigenwave phase Φ is Lorentz invariant, to set all these parameters, one can conveniently use the four-dimensional wave vector $\mathbf{K}$, the field tensor F, and the so-called beam manifold (BM) $\mathcal{B}$ [23,24]. This approach provides Lorentz covariant parametrization for an electromagnetic plane-wave superposition as

$$F(\mathbf{x})=\int_{\mathcal{B}}e^{i\Phi(\mathbf{x},b)}F(b)u(b)d\mathcal{B}, \tag{6}$$

where

$$\Phi(\mathbf{x},b)=\mathbf{x}\cdot\mathbf{K}(b)+\Phi_0(b) \tag{7}$$

is the phase of a partial eigenwave, $\Phi_0(b)$ is the initial phase (the phase value at the point $\mathbf{x}=0$), $F(b)$ is the normalized real or complex amplitude specifying the eigenwave polarization, $u=u(b)$ is a scalar real function on $\mathcal{B}$, specifying the eigenwave magnitude, and $d\mathcal{B}$ is the infinitesimal element of $\mathcal{B}$.

3. Wave-vector manifold $\mathcal{K}$

The wave-vector manifold (WVM) is the image $\mathcal{K}$ of $\mathcal{B}$ under the mapping $b\mapsto\mathbf{K}(b)$, i.e., it is the subset $\{\mathbf{K}(b);\ b\in\mathcal{B}\}$ of the four-dimensional wave-vector space. The mapping $\mathbf{K}$ of $\mathcal{B}$ onto $\mathcal{K}=\mathbf{K}(\mathcal{B})$ need not be injective (one-one). Since we treat here the electromagnetic plane-wave superpositions in vacuum, any point $\mathbf{K}(b)=\mathbf{k}(b)+\mathbf{e}_4\omega(b)/c$ of the WVM satisfies the dispersion equation $[\mathbf{K}(b)]^2=0$, i.e., $[\mathbf{k}(b)]^2=[\omega(b)/c]^2$.

4. Initial phase function Φ_0 and zero phase manifold $\mathcal{Z}$

Since the functions $\mathbf{K}=\mathbf{K}(b)$, $F=F(b)$, $u=u(b)$, and $\Phi_0=\Phi_0(b)$ are independent of $\mathbf{x}$, the field pattern in a particular space-time domain, described by the values $F(\mathbf{x})$ [Eq. (6)] of the two-form F, is dictated by phases of eigenwaves in this domain. In other words, the field value $F(\mathbf{x}_1)$ at any given space-time point $\mathbf{x}_1$ is dictated by the local phase function $\Phi_1=\Phi_1(b)=\Phi(\mathbf{x}_1,b)$. If the phase functions Φ_1 and Φ_2 at the points $\mathbf{x}_1$ and $\mathbf{x}_2$ are related as $\Phi_2-\Phi_1\equiv\mathbf{K}(b)\cdot(\mathbf{x}_2-\mathbf{x}_1)=2\pi n$, where n is an integer, the field values in these points coincide: $F(\mathbf{x}_2)=F(\mathbf{x}_1)$.

By changing initial phases of partial eigenwaves, one can obtain an infinite family of different, but closely related fields that can be treated as different phase states of the same plane-wave superposition. All members of this family are described by the same functions $\mathbf{K}=\mathbf{K}(b)$, $F=F(b)$, $u=u(b)$ on $\mathcal{B}$, but they are distinguished by different initial

phase functions (IPFs) $\Phi_0=\Phi_0(b)$ on the same BM $\mathcal{B}$. In particular, the field $F'(\mathbf{x})=F(\mathbf{x}-\mathbf{y})$, obtained from the field $F(\mathbf{x})$ [Eq. (6)] by a space-time shift $\mathbf{y}$, is described by the IPF $\Phi_0'=\Phi_0(b)-\mathbf{y}\cdot\mathbf{K}(b)$.

The functions $\mathbf{K}=\mathbf{K}(b)$ and $\Phi_0=\Phi_0(b)$ in Eq. (7) can be set independently of each other. Alternatively, one can use the parametrization

$$\Phi(\mathbf{x},b)=\mathbf{K}(b)\cdot[\mathbf{x}-\mathbf{x}_p(b)], \tag{8}$$

where $\mathbf{x}_p=\mathbf{x}_p(b)$ is a vector real function on $\mathcal{B}$, specifying the IPF as $\Phi_0=-\mathbf{K}(b)\cdot\mathbf{x}_p(b)$. The image $\mathcal{Z}$ of $\mathcal{B}$ under the mapping $b\mapsto\mathbf{x}_p(b)$ is the subset $\{\mathbf{x}_p(b);\ b\in\mathcal{B}\}$ of the Minkowski space. Since $\Phi(\mathbf{x}_p(b),b)=0$ for any $b\in\mathcal{B}$, $\mathcal{Z}$ is called below the zero phase manifold (ZPM). In other words, $F(b)u(b)d\mathcal{B}$ is the field value of the infinitesimal eigenwave at the point $\mathbf{x}=\mathbf{x}_p(b)$. With a given ZPM, the IPF Φ_0 is uniquely defined by the wave-vector function $\mathbf{K}=\mathbf{K}(b)$.

Both manifolds $\mathcal{B}$ and $\mathcal{Z}$ are the Lorentz invariant identifying geometrical characteristics of each field under consideration. However, in contrast to $\mathcal{Z}$, $\mathcal{B}$ is not related directly with the space-time. It is merely a parametrization manifold, i.e., each point b of $\mathcal{B}$ specifies the corresponding eigenwave, and the infinitesimal element $d\mathcal{B}$ is a Lorentz scalar invariant by definition. The four-dimensional formalism is especially useful in the investigation of localized electromagnetic and weak gravitational fields moving without dispersing at speed $V<c$ [23,24], as well as in analysis of relativistic particle movement in localized fields (see Sec. VI B).

Using the relations $\mathbf{x}=\mathbf{r}+ct\mathbf{e}_4$, $\mathbf{x}_p=\mathbf{r}_p+ct_p\mathbf{e}_4$, and $\mathbf{K}=\mathbf{k}+\mathbf{e}_4\omega/c$, we can present the eigenwave phase as

$$\Phi(\mathbf{x},b)=\Phi(\mathbf{r},t,b)=\mathbf{k}(b)\cdot[\mathbf{r}-\mathbf{r}_p(b)]-\omega(b)[t-t_p(b)]. \tag{9}$$

Thus, in the frame L, the ZPM is described by a vector function $\mathbf{r}_p=\mathbf{r}_p(b)$ and a scalar function $t_p=t_p(b)$, specifying the spatial and the temporal eigenwave shifts, respectively. In the special case, when the field is time harmonic (THF) in some Lorentz frame, for example, $\omega(b)\equiv\omega$ in the frame L, it is convenient to set the ZPM so as to obtain $t_p(b)\equiv 0$.

5. Polarization manifold $\mathcal{P}$

Let $\mathbf{v}_a\in V$ be an auxiliary vector related to the contravariant $\mathbf{K}$ and the covariant $K=g\cdot\mathbf{K}$ wave vectors by the normalization condition $\mathbf{v}_a\cdot\mathbf{K}=\mathbf{v}_a\rfloor K=1$. The eigenwave two-form F and two-vector $\mathbf{F}$ can be written as [29,30]

$$F=K\wedge f, \quad \mathbf{F}=\mathbf{K}\wedge\mathbf{f}, \tag{10}$$

where $f=\mathbf{v}_a\rfloor F$ and $\mathbf{f}=g^{-1}\cdot f$ are the covariant and contravariant polarization vectors satisfying the condition $\mathbf{K}\rfloor f\equiv\mathbf{f}\rfloor K=0$. Thus, to set the normalized amplitude function $F=F(b)$ in Eq. (6), it is sufficient to set either the covariant $f=f(b)$ or contravariant $\mathbf{f}=\mathbf{f}(b)$ vector function on the BM. Like $\mathcal{Z}$, the image $\mathcal{P}$ of $\mathcal{B}$ under the mapping $b\mapsto\mathbf{f}(b)$ is the subset $\{\mathbf{f}(b);\ b\in\mathcal{B}\}$ of the Minkowski space. Since $\mathcal{P}$ provides the Lorentz invariant geometrical characteristic of partial eigenwaves polarization states, it is called below the polarization manifold (PM).

It should be noted that the transformation $\mathbf{f}\mapsto\mathbf{f}'=\mathbf{f}+\alpha\mathbf{K}$ does not change $\mathbf{F}$ at any given scalar α, because $\mathbf{K}\rfloor K=0$ and $\mathbf{K}\wedge\mathbf{K}=0$. It is merely equivalent to the replacement of the auxiliary vector parameter $\mathbf{v}_a$ by some other vector $\mathbf{v}_a'$ satisfying the conditions $\mathbf{v}_a'\cdot\mathbf{K}=1$ and $\mathbf{v}_a'\cdot\mathbf{f}'=0$. Naturally, the auxiliary vector $\mathbf{v}_a$ can be chosen so as to obtain $\mathbf{f}$ with a specific physical meaning in the frame L. In particular, to describe the eigenwave polarization in terms of the electric field in the frame L, we chose $\mathbf{v}_a=-\mathbf{e}_4/k$. Then, $\mathbf{f}=\mathbf{E}/k$, and we obtain

$$\mathbf{F}=(\hat{\mathbf{k}}+\mathbf{e}_4)\wedge\mathbf{E}. \tag{11}$$

In this frame, the PM is defined by the function $\mathbf{E}=\mathbf{E}(b)$ on $\mathcal{B}$, where $\hat{\mathbf{k}}(b)\cdot\mathbf{E}(b)=0$ for any $b\in\mathcal{B}$, $\mathbf{E}\cdot\mathbf{E}^*=1$, and $\mathbf{E}^*$ is complex conjugate of $\mathbf{E}$.

6. Magnitude function u and magnitude manifold $\mathcal{M}$

The infinitesimal eigenwave with the wave vector $\mathbf{K}(b)$ has the amplitude $F(b)u(b)d\mathcal{B}$. This factorization makes it possible to set the polarization and the magnitude of this wave by two independent factors, i.e., the two-form $F(b)$ and the scalar $u(b)$, respectively. That is why the magnitude function (MF), $u=u(b)$, plays a major role in setting the contribution of each eigenwave to the total field, even though $d\mathcal{B}$ also may depend on b. We assume that $u(b)$ is nonvanishing almost everywhere, i.e., for all $b\in\mathcal{B}$ with allowable exception of a set of measure zero in $\mathcal{B}$. Otherwise, the BM is actually the domain of $\mathcal{B}$ with nonzero $u(b)$.

7. Covariant field design

In the frame of the presented covariant approach, a superposition of homogeneous eigenwaves in the source-free space is defined by the functions $\mathbf{K}=\mathbf{K}(b)$, $\mathbf{x}_p=\mathbf{x}_p(b)$ [or $\Phi_0=\Phi_0(b)$], $\mathbf{f}=\mathbf{f}(b)$, and $u=u(b)$ on the beam manifold $\mathcal{B}$. All these functions as well as the related geometrical objects—the beam manifold $\mathcal{B}$ and its images $\mathcal{K}$, $\mathcal{P}$, and $\mathcal{Z}$—are Lorentz invariant characteristics of the field. Except for the only condition $\mathbf{K}(b)\cdot\mathbf{f}(b)=0$ imposed on the points of $\mathcal{K}$ and $\mathcal{P}$, the described design characteristics can be set independently from each other in any convenient reference frame.

On the whole, the field base (the set of eigenwaves forming the field) is specified by the function $\mathbf{K}=\mathbf{K}(b)$, whereas a field state is given by the functions $\mathbf{f}=\mathbf{f}(b)$, $\mathbf{x}_p=\mathbf{x}_p(b)$, and $u=u(b)$. The manifolds $\mathcal{K},\mathcal{P},\mathcal{Z}$ provide a graphic portrayal of this field.

B. Three-dimensional parametrization

1. Time harmonic and evolving fields

If the field under consideration is time harmonic in some reference frame L, this frame naturally becomes preferable for its description and parametrization. In particular, instead of the four-dimensional vector functions $\mathbf{K}=\mathbf{K}(b)$, $\mathbf{f}=\mathbf{f}(b)$,

and $\mathbf{x}_p=\mathbf{x}_p(b)$, one can describe this field by the three-dimensional vector functions $\mathbf{k}=\mathbf{k}(b)$, $\mathbf{E}=\mathbf{E}(b)$, and $\mathbf{r}_p=\mathbf{r}_p(b)$. Correspondingly, instead of the manifolds $\mathcal{K},\mathcal{P},\mathcal{Z}$ in the Minkowski space, one can characterize the THF by their sections $\mathcal{K}_3$, $\mathcal{P}_3$, and $\mathcal{Z}_3$, lying in the Euclidean subspace in the frame L.

In the present paper, we confine our numerical illustrations mainly to the time-harmonic beams $[\omega(b)\equiv\omega]$

$$\mathbf{W}(\mathbf{r},t)=\int_{\mathcal{B}} e^{i\Phi(\mathbf{r},t,b)}u(b)\mathbf{W}(b)d\mathcal{B} \tag{12}$$

with two-dimensional $\mathcal{B}$. However, the presented approach can be readily extended to the beams

$$\check{\mathbf{W}}(\mathbf{r},t)=\int_{\check{\mathcal{B}}} e^{i\Phi(\mathbf{r},t,b)}j_0[p\Phi(\mathbf{r},t,b)]\mathbf{W}(b)u(b)d\mathcal{B} \tag{13}$$

with three-dimensional beam manifold $\check{\mathcal{B}}=\mathcal{B}\times[k_-,k_+]$. Here, $\mathbf{W}$ is the electric $\mathbf{E}$ or magnetic $\mathbf{B}$ field vector, j_0 is the spherical Bessel function, $p=\Delta k/k$, $\Delta k=(k_+-k_-)/2$, and $k=(k_++k_-)/2$. The solutions $\check{\mathbf{W}}(\mathbf{r},t)$, related to $\mathbf{W}(\mathbf{r},t)$ [Eq. (12)] by integration over wave number k as

$$\check{\mathbf{W}}(\mathbf{r},t)=\frac{1}{2\Delta k}\int_{k_-}^{k_+}\mathbf{W}(\mathbf{r},t)dk, \tag{14}$$

describe finite-energy evolving fields [24]. In the case of quasimonochromatic beams, $\Delta k\ll k$.

One can carry out orthogonal transformations (rotations, reflections, and their compositions) and spatial shifts (translations) of these fields by the corresponding transformations of $\mathcal{K}_3$, $\mathcal{P}_3$, and $\mathcal{Z}_3$ as follows. The field $\mathbf{W}_1(\mathbf{r},t)=G_0\mathbf{W}(\tilde{G}_0\mathbf{r},t)$ is obtained from $\mathbf{W}(\mathbf{r},t)$ by making use of an orthogonal operator G_0. The latter satisfies the condition $G_0^{-1}=\tilde{G}_0$, where $\tilde{G}_0$ is the transposed operator. The field $\mathbf{W}_1$ is obtained by the orthonormal transformations of $\mathcal{K}_3$, $\mathcal{P}_3$, and $\mathcal{Z}_3$, described by the mappings $\mathbf{k}(b)\mapsto G_0\mathbf{k}(b)$, $\mathbf{W}(b)\mapsto G_0\mathbf{W}(b)$, and $\mathbf{r}_p(b)\mapsto G_0\mathbf{r}_p(b)$, respectively. Similarly, the shifted field $\mathbf{W}_2(\mathbf{r},t)=\mathbf{W}(\mathbf{r}-\mathbf{r}_0,t)$ results from the shift $\mathbf{r}_0$ of the $\mathcal{Z}_3$, described by the mapping $\mathbf{r}_p(b)\mapsto\mathbf{r}_p(b)+\mathbf{r}_0$. It is essential that this transformation is independent of the WVM $\mathcal{K}_3$. The same shift can also be induced by the IPF transformation $\Phi_0(b)\mapsto\Phi_0(b)-\mathbf{k}(b)\cdot\mathbf{r}_0$ that depends on both functions $\Phi_0=\Phi(b)$ and $\mathbf{k}=\mathbf{k}(b)$.

2. Standing waves defined by the spherical harmonics Y_j^s

By way of illustration, let us consider the three-dimensional standing electromagnetic waves presented in Refs. [22–24]. They are defined by the spherical harmonics (Y_j^s) as

$$\mathbf{E}_j^s(\mathbf{r},t)=u_0e^{-i\omega t}\int_0^{2\pi}d\varphi\int_0^{\pi}e^{i\mathbf{k}(\theta,\varphi)\cdot\mathbf{r}}Y_j^s(\theta,\varphi)\times\mathbf{E}(\theta,\varphi)\sin\theta d\theta, \tag{15}$$

where

$$Y_j^s(\theta,\varphi)=N_{js}P_j^{|s|}(\cos\theta)e^{is\varphi}, \tag{16}$$

$$N_{js}=\sqrt{\frac{(2j+1)(j-|s|)!}{4\pi(j+|s|)!}}, \tag{17}$$

and $P_j^s(\cos\theta)$ is the spherical Legendre function, u_0 is some normalizing constant factor. For these waves, the beam manifold $\mathcal{B}$ is the unit sphere S^2, and $d\mathcal{B}=\sin\theta d\theta d\varphi$.

To set the functions $\mathbf{k}=\mathbf{k}(\theta,\varphi)$ and $\mathbf{E}=\mathbf{E}(\theta,\varphi)$, i.e., propagation directions and polarizations of eigenwaves, one can use the spherical basis vectors

$$\mathbf{e}_r(\theta,\varphi)=\mathbf{e}_R(\varphi)\sin\theta+\mathbf{e}_3\cos\theta, \tag{18a}$$

$$\mathbf{e}_M(\theta,\varphi)=\mathbf{e}_R(\varphi)\cos\theta-\mathbf{e}_3\sin\theta, \tag{18b}$$

$$\mathbf{e}_A(\varphi)=-\mathbf{e}_1\sin\varphi+\mathbf{e}_2\cos\varphi, \tag{18c}$$

where

$$\mathbf{e}_R(\varphi)=\mathbf{e}_1\cos\varphi+\mathbf{e}_2\sin\varphi. \tag{19}$$

In Refs. [23,24], we have treated the standing waves with $\mathbf{k}(\theta,\varphi)=k\mathbf{e}_r$ and two different polarization states, namely, E_M fields with the meridional orientation $[\mathbf{E}(\theta,\varphi)=\mathbf{e}_M]$ and E_A fields with the azimuthal orientation $[\mathbf{E}(\theta,\varphi)=\mathbf{e}_A]$ of the eigenwave electric field. They are formed from plane waves of all possible propagation directions. The family of these waves consists of storms, defined by the zonal spherical harmonics Y_j^0, and whirls defined by the other Y_j^s $(s\neq0)$. For the storms, the time average energy flux is identically zero at all points. The whirls have circular energy flux lines lying in the planes orthogonal to $\mathbf{e}_3$.

For these fields, the WVM $\mathcal{K}_3$ is merely the sphere S_k^2 with a radius $k=\omega/c$ in the three-dimensional wave-vector space, and $\hat{\mathbf{k}}(\theta,\varphi)\equiv\mathbf{e}_r(\theta,\varphi)$. For various types of time-harmonic orthonormal beams also treated in Refs. [23,24], the WVM is some domain of S_k^2. The PM $\mathcal{P}_3$ for E_M and E_A fields can be conveniently illustrated as the meridional and azimuthal unit vector fields on the surface of this sphere, respectively.

The ZPM $\mathcal{Z}_3$ is described by the relations

$$t_p\equiv0,\quad \mathbf{r}_p(\theta,\varphi)=-\frac{s\varphi}{k}\mathbf{e}_r(\theta,\varphi), \tag{20}$$

where $\theta\in[0,\pi]$ and $\varphi\in[0,2\pi]$. It can be rewritten in terms of dimensionless radius vector $\mathbf{r}_p'=\mathbf{r}_p/\lambda=x_p'\mathbf{e}_1+y_p'\mathbf{e}_2+z_p'\mathbf{e}_3$ as

$$\mathbf{r}_p'=-\frac{s\varphi}{2\pi}\mathbf{e}_r(\theta,\varphi). \tag{21}$$

The corresponding normalized zero phase manifold $\mathcal{Z}_3$ (in this case, it is a parametrized surface) is independent of j, and its dimensions are proportional to s. For the electromagnetic storms $(s=0)$, the ZPM shrinks to the point $\mathbf{r}_p'=0$.

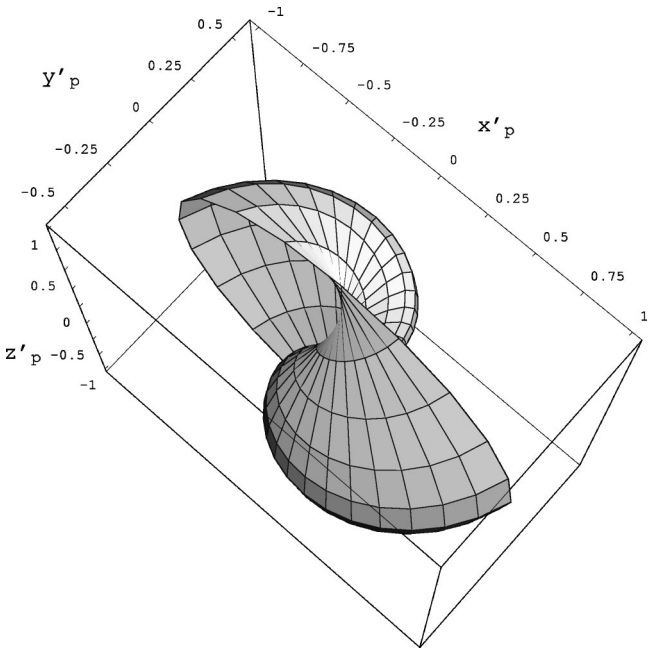

FIG. 1. Zero phase manifold of electromagnetic whirls defined by the spherical harmonics Y_j^2; $j=2,3,\ldots$.

Since, at any integer n, the phase shift $2\pi n$ does not change the eigenwave field, one can replace Eq. (21) by the equation

$$\mathbf{r}_p' = -\left\{\frac{s\varphi}{2\pi}\right\}\mathbf{e}_r(\theta,\varphi), \tag{22}$$

where $\{x\}$ denotes the fractional part of a number x, defined as a odd numerical function, for example, $\{\pm 2.4\}=\pm 0.4$. In this case, the whole $\mathcal{Z}_3$ lies within the unit sphere. Figure 1 shows the corresponding ZPM of electromagnetic whirls, defined by the spherical harmonics Y_j^2; $j=2,3,\ldots$.

The same approach, based on the use of $\mathbf{r}_p(b)$ parallel to $\mathbf{k}(b)$, can be applied to redefine any other ZPM $\mathcal{Z}_3$. The transverse component of $\mathbf{r}_p(b)$ [orthogonal to $\mathbf{k}(b)$] does not contribute to $\Phi_0(b)$. Given the WVM $\mathcal{K}_3$, one can redefine any ZPM $\mathcal{Z}_3$ to satisfy the condition $\mathbf{r}_p(b)\|\mathbf{k}(b)$. In this case $\mathbf{r}_p'(b)=-\Phi_0(b)\hat{\mathbf{k}}(b)/2\pi$ graphically illustrates the dependence of the initial phase Φ_0 on the propagation direction $\hat{\mathbf{k}}$.

It is significant that both conditions $\mathbf{r}_p(b)\|\mathbf{k}(b)$ and $|\Phi_0|\in[0,2\pi]$ are not mandatory. In some cases, they become inconvenient and can be canceled, for example, to introduce (independently from $\mathcal{K}_3$) a large continuous ZPM $\mathcal{Z}_3$ or to describe some field transformation, such as a spatial shift $\mathbf{r}_0$ with $\mathbf{r}_0^2>\lambda^2$ (see Sec. II B 1).

Let us now consider magnitude functions of the standing waves under the consideration. It follows from Eqs. (15) and (16) that the MF of the wave $\mathbf{E}_j^s$ has the form

$$u = u_0 N_{js} P_j^{|s|}(\cos\theta) \tag{23}$$

and can be graphically illustrated by a parametrized surface as

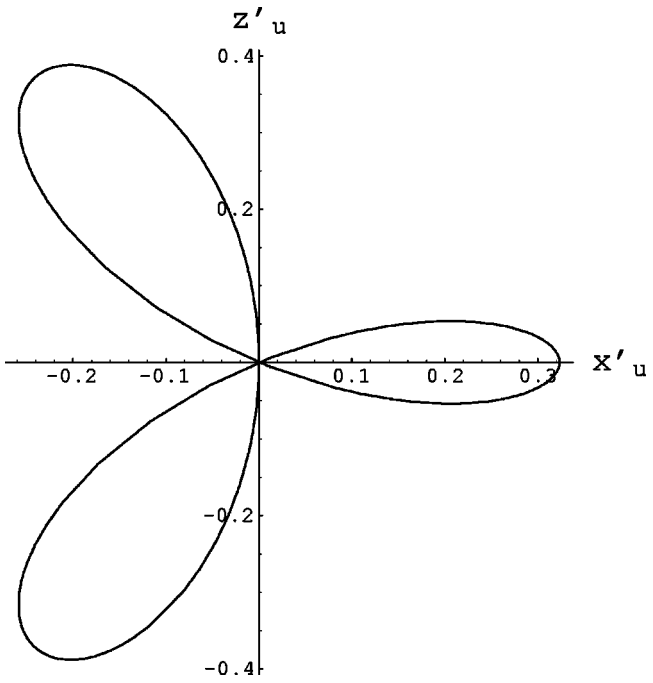

FIG. 2. Directional diagram of the electromagnetic whirl defined by the spherical harmonics Y_3^1.

$$\mathbf{r}_u' = (u/u_0)\mathbf{e}_r(\theta,\varphi) = N_{js}P_j^{|s|}(\cos\theta)\mathbf{e}_r(\theta,\varphi), \tag{24}$$

where $\theta\in[0,\pi]$ and $\varphi\in[0,2\pi]$. Since this surface is axially symmetric, it is sufficient to depict its section by a meridional plane $\varphi=0$. This gives the directional diagram, i.e., the dependence of the eigenwave magnitude on the propagation direction, as

$$\mathbf{r}_u' = x_u'\mathbf{e}_1 + z_u'\mathbf{e}_3 = N_{js}P_j^{|s|}(\cos\theta)(\mathbf{e}_1\cos\theta + \mathbf{e}_3\sin\theta), \tag{25}$$

where $\theta\in[0,\pi]$. It should be mentioned that the MF u [Eq. (23)] may take negative values at some intervals of θ. Alternatively, one can replace u by its absolute value $|u|$ and introduce an additional phase shift π whenever u becomes negative. However, this is an unnecessary complication that breaks the continuity of the ZPM and makes it dependent on the degree j of Y_j^s. Figure 2 illustrates the directional diagram of the electromagnetic whirl defined by the spherical harmonics Y_3^1. The lobes lying in the second and third quadrants correspond to the negative values of the MF. Figure 7 in Ref. [23] depicts the only nonvanishing (azimuthal) component of the energy flux vector of this whirl.

III. FIELDS DEFINED BY THE ROTATION GROUP

In our previous works [22–24], we have treated linear fields defined by a given set of orthonormal scalar functions on a two-dimensional or three-dimensional beam manifold. In this section, we present a different type of plane-wave superpositions—electromagnetic fields defined by the rotation group. For the sake of brevity, we confine our consideration to the time-harmonic superpositions of linearly polarized homogeneous plane waves in vacuum, that can be

parametrized by points $b \in \mathcal{B}$ of a two-dimensional BM as follows:

$$\mathbf{W}(\mathbf{r},t)=e^{-i\omega t}\int_{\mathcal{B}} e^{i\mathbf{k}(b)\cdot[\mathbf{r}-\mathbf{r}_p(b)]}\mathbf{W}(b)u(b)d\mathcal{B}. \quad (26)$$

As before, the unit real vectors $\mathbf{W}(b)=\mathbf{E}(b)$ and $\mathbf{W}(b)=\mathbf{B}(b)$ specify the polarization in terms of the electric and the magnetic fields, respectively, whereas the eigenwave magnitude is defined by the MF $u=u(b)$. In concordance with Maxwell's equations, the normalized amplitudes $\mathbf{E}(b)$ and $\mathbf{B}(b)$ of each eigenwave are related as

$$\mathbf{B}(b)=\hat{\mathbf{k}}(b)\times\mathbf{E}(b). \quad (27)$$

For the plane-wave superposition under consideration, the orthonormal triads $[\hat{\mathbf{k}}(b),\mathbf{E}(b),\mathbf{B}(b)]$ of any pair of partial eigenwaves are related by a rotation operator. Let us denote $\hat{\mathbf{k}}_0=\hat{\mathbf{k}}(b_0)$, $\mathbf{E}_0=\mathbf{E}(b_0)$, and $\mathbf{B}_0=\mathbf{B}(b_0)$, where $b_0 \in \mathcal{B}$ is an arbitrarily given point of the BM. Then, we can set the triads of all eigenwaves by a rotation operator function $G=G(b)$ as

$$\hat{\mathbf{k}}(b)=G(b)\hat{\mathbf{k}}_0, \quad \mathbf{E}(b)=G(b)\mathbf{E}_0, \quad \mathbf{B}(b)=G(b)\mathbf{B}_0, \quad (28)$$

where $G(b_0)=\mathbb{1}$ is the unit dyadic. In its turn, the rotation operator G can be conveniently parametrized by the Euler angles or the Fedorov complex vector parameter [31].

This approach makes it possible to describe the beam by the evolution operator,

$$\mathcal{F}(\mathbf{r},t)=e^{-i\omega t}\int_{\mathcal{B}} e^{i\mathbf{k}(b)\cdot[\mathbf{r}-\mathbf{r}_p(b)]}u(b)G(b)d\mathcal{B}, \quad (29)$$

that defines both the electric and magnetic fields as

$$\mathbf{E}(\mathbf{r},t)=\mathcal{F}(\mathbf{r},t)\mathbf{E}_0, \quad \mathbf{B}(\mathbf{r},t)=\mathcal{F}(\mathbf{r},t)\mathbf{B}_0. \quad (30)$$

It should be noted that Eqs. (29) and (30) can be readily applied to superpositions of eigenwaves with elliptic or circular polarization. To this end, it is sufficient to set the normalized amplitudes $\mathbf{E}_0$ and $\mathbf{B}_0$ as

$$\mathbf{E}_0=\mathbf{a}+i\mathbf{b}, \quad \mathbf{B}_0=\hat{\mathbf{k}}_0\times\mathbf{E}_0, \quad (31)$$

where $\mathbf{a}$ and $\mathbf{b}$ are the major and the minor semiaxes, $\mathbf{a}\cdot\hat{\mathbf{k}}_0=\mathbf{b}\cdot\hat{\mathbf{k}}_0=\mathbf{a}\cdot\mathbf{b}=0$, $\mathbf{a}^2+\mathbf{b}^2=1$, and $\mathbf{a}^2-\mathbf{b}^2\geqslant 0$. Beams in isotropic media, including chiral ones, can be treated similarly, except that the eigenwaves in an isotropic chiral medium are circularly polarized ($\mathbf{a}^2=\mathbf{b}^2$). Superpositions of eigenwaves with different polarizations can be treated by making use of the exponential evolution operators [32].

The operator G of rotation through the angle φ around the unit vector $\mathbf{n}$ can be written as

$$G\equiv\exp(\varphi\mathbf{n}^{\times})=\mathbf{n}\otimes\mathbf{n}+(\mathbb{1}-\mathbf{n}\otimes\mathbf{n})\cos\varphi+\mathbf{n}^{\times}\sin\varphi, \quad (32)$$

where $\mathbf{n}^{\times}$ is the antisymmetric tensor dual to $\mathbf{n}$ ($\mathbf{n}^{\times}\mathbf{E}=\mathbf{n}\times\mathbf{E}$). In this paper, we shall parametrize the operator G by three rotation angles (ψ_j, $j=1,2,3$) as

$$G=\exp(\psi_3\mathbf{d}^{\times})\exp(\psi_2\mathbf{e}_A^{\times})\exp(\psi_1\mathbf{e}_3^{\times}), \quad (33)$$

where

$$\mathbf{d}=\exp(\psi_2\mathbf{e}_A^{\times})\exp(\psi_1\mathbf{e}_3^{\times})\mathbf{d}_0, \quad (34)$$

$\mathbf{e}_A=\mathbf{e}_A(\psi_1)$, and $\mathbf{d}_0$ is a unit vector that will be specified in subsequent sections.

In particular, if $\mathbf{d}_0=\mathbf{e}_3$, the operator G can be written as

$$G=\mathbf{g}_1\otimes\mathbf{e}_1+\mathbf{g}_2\otimes\mathbf{e}_2+\mathbf{d}\otimes\mathbf{e}_3, \quad (35)$$

where

$$\mathbf{g}_1=\mathbf{e}_M(\psi_2,\psi_1)\cos\psi_3+\mathbf{e}_A(\psi_1)\sin\psi_3, \quad (36a)$$

$$\mathbf{g}_2=-\mathbf{e}_M(\psi_2,\psi_1)\sin\psi_3+\mathbf{e}_A(\psi_1)\cos\psi_3, \quad (36b)$$

$$\mathbf{d}=\mathbf{e}_r(\psi_2,\psi_1)=\mathbf{e}_R(\psi_1)\sin\psi_2+\mathbf{e}_3\cos\psi_2. \quad (36c)$$

The operator function $G=G(b)$ can be uniquely defined by three real scalar functions $\psi=\psi_j(b)$, $j=1,2,3$. In particular, for the E_M and E_A fields defined by the spherical harmonics (see Sec. II B 2), $\mathbf{E}_0=\mathbf{e}_1$ and $\mathbf{E}_0=\mathbf{e}_2$, respectively. In both cases, $\hat{\mathbf{k}}_0=\mathbf{e}_3$, $\psi_1=\varphi$, $\psi_2=\theta$, and $\psi_3\equiv 0$.

All three-dimensional standing waves defined by the spherical harmonics have the same BM (the unit sphere $\mathcal{B}=S^2$) as well as the same WVM (the sphere $\mathcal{K}_3=S_k^2$). Although E_M and E_A waves have different PMs ($\mathcal{P}_3$ is set by the meridional and the azimuthal vectors, respectively), their electric and magnetic fields are related by the duality transformation. The diversity of the standing waves $\mathbf{E}_j^s$ is caused mainly by various MFs u [Eq. (23)] and different ZMPs $\mathcal{Z}_3$ (see Fig. 1). However, $\mathcal{Z}_3$ depends only on s that acts as scaling multiplier [see Eq. (20)].

The THF defined by the rotation group possess a much larger diversification potential. To illustrate this, let us present two types of such fields with topologically different beam manifolds—spherical and toroidal BMs. For the sake of brevity, we consider here only a rather special case when the MF u reduces to a constant u_0.

IV. FIELD WITH SPHERICAL BM

Let the BM be the unit sphere ($\mathcal{B}=S^2$) and $u(\theta,\varphi)\equiv u_0$. In this case, the evolution operator $\mathcal{F}$ [Eq. (29)] becomes

$$\mathcal{F}(\mathbf{r},t)=u_0e^{-i\omega t}\int_0^{2\pi}d\varphi\int_0^{\pi}e^{i\Phi(\mathbf{r},\theta,\varphi)}G(\theta,\varphi)\sin\theta d\theta, \quad (37)$$

where

$$\Phi(\mathbf{r},\theta,\varphi)=2\pi\hat{\mathbf{k}}(\theta,\varphi)\cdot[\mathbf{r}'-\mathbf{r}'_p(\theta,\varphi)], \quad \mathbf{r}'=\mathbf{r}/\lambda. \quad (38)$$

As an example of the ZPM $\mathcal{Z}_3$, let us consider an ellipsoidal surface that, in terms of the dimensionless radius vector $\mathbf{r}'_p=\mathbf{r}_p/\lambda$, is described as

$$\mathbf{r}'_p=(\mathbf{e}_1R_1\cos\varphi_1+\mathbf{e}_2R_2\sin\varphi_1)\sin\varphi_2+\mathbf{e}_3R_3\cos\varphi_2, \tag{39}$$

where R_1, R_2, and R_3 are the semiaxes, $\varphi_1\in[0,2\pi]$ and $\varphi_2\in[0,\pi]$.

Let us confine our illustrations to the case of linear functions φ_j [Eq. (39)] and ψ_j [Eq. (33)], given as

$$\varphi_j=\theta b_{1j}+\varphi b_{2j}+b_{3j}, \quad j=1,2, \tag{40a}$$

$$\psi_j=\theta c_{1j}+\varphi c_{2j}+c_{3j}, \quad j=1,2,3, \tag{40b}$$

where b_{ij} and c_{ij} are some given real coefficients.

Even within the imposed restrictions, a multitude of design possibilities still remains. One can construct various families of localized fields by setting the PM and the WVM through the parameters $\mathbf{E}_0$, $\hat{\mathbf{k}}_0$, $\mathbf{d}_0$, (b_{ij}), and the ZPM through the parameters R_1, R_2, R_3, and (c_{ij}). It is essential that the mapping and $\mathbf{r}'_p=\mathbf{r}'_p(\theta,\varphi)$ need not be injective (one-one) and/or surjective (onto). In other words, the ZPM $\mathcal{Z}_3$ may be a domain of or a curve on the described ellipsoidal surface. The special case $R_1=R_2=R_3$, when the ZPM shrinks to the point $\mathbf{r}'_p=0$, is also allowable. Let us present a few graphic illustrations.

A. Fields with $\psi_3\equiv 0$

Let us set $\varphi_1=\psi_1=\varphi\in[0,2\pi]$, $\varphi_2=\psi_2=\theta\in[0,\pi]$, and $\psi_3=0$. In this case, the rotation operator $G(\theta,\varphi)$ becomes

$$G(\theta,\varphi)=\exp[\theta\mathbf{e}_A^{\times}(\varphi)]\exp(\varphi\mathbf{e}_3^{\times})=\mathbf{e}_M\otimes\mathbf{e}_1+\mathbf{e}_A\otimes\mathbf{e}_2+\mathbf{e}_r\otimes\mathbf{e}_3. \tag{41}$$

It follows from Eqs. (32) and (41) that this operator satisfies the relations

$$G_0G(\theta,\varphi)G_0=G(-\theta,\varphi), \tag{42a}$$

$$G_1G(\theta,\varphi)=G(\theta,\varphi+\varphi_0), \tag{42b}$$

where $G_0=\mathbb{1}-2\mathbf{e}_3\otimes\mathbf{e}_3$ is the operator of reflection in the plane normal to $\mathbf{e}_3$, and $G_1=\exp(\varphi_0\mathbf{e}_3^{\times})$ is the operator of rotation through an arbitrary angle φ_0 around the vector $\mathbf{e}_3$.

Let us set $\mathbf{k}_0=\mathbf{e}_3$. Then, the basis functions for E_M and E_A fields, composed of eigenwaves with the meridional $[\mathbf{E}(\theta,\varphi)=\mathbf{e}_M]$ and the azimuthal $[\mathbf{E}(\theta,\varphi)=\mathbf{e}_A]$ orientations of the electric field $\mathbf{E}$, can be defined as

$$\mathbf{W}_1=\mathcal{F}(\mathbf{r},t)\mathbf{e}_1, \quad \mathbf{W}_2=\mathcal{F}(\mathbf{r},t)\mathbf{e}_2. \tag{43}$$

The electric and magnetic fields of E_M ($\mathbf{E}_0=\mathbf{e}_1$) and E_A ($\mathbf{E}_0=\mathbf{e}_2$) fields are related by the duality transformation as

$$\mathbf{E}_M=-\mathbf{B}_A=\mathbf{W}_1, \quad \mathbf{B}_M=\mathbf{E}_A=\mathbf{W}_2. \tag{44}$$

If the localized field is composed of eigenwaves with different polarization states [see Eq. (31)], i.e., $\mathbf{E}_0=E_{01}\mathbf{e}_1+E_{02}\mathbf{e}_2$, it can be described as a superposition of E_M and E_A fields,

$$\mathbf{E}=E_{01}\mathbf{W}_1+E_{02}\mathbf{W}_2, \quad \mathbf{B}=E_{01}\mathbf{W}_2-E_{02}\mathbf{W}_1. \tag{45}$$

Since $G_0\mathbf{r}'_p(\theta,\varphi)=\mathbf{r}'_p(\pi-\theta,\varphi)$, and $G(\theta,\varphi)$ satisfies the relation (42a), the functions $\mathbf{W}_1$ and $\mathbf{W}_2$ have the following symmetry properties:

$$\mathbf{W}_1(G_0\mathbf{r},t)=-G_0\mathbf{W}_1(\mathbf{r},t), \tag{46a}$$

$$\mathbf{W}_2(G_0\mathbf{r},t)=G_0\mathbf{W}_2(\mathbf{r},t). \tag{46b}$$

To obtain an axially symmetric field, it is sufficient to set $R_2=R_1$ in Eq. (39). In this case, the ZPM becomes an ellipsoid of revolution, i.e., $G_1\mathbf{r}'_p(\theta,\varphi)=\mathbf{r}'_p(\theta,\varphi+\varphi_0)$. From Eqs. (28) and (42b), we obtain the similar relation for $\hat{\mathbf{k}}$: $G_1\hat{\mathbf{k}}(\theta,\varphi)=\hat{\mathbf{k}}(\theta,\varphi+\varphi_0)$. All this results in the following symmetry relations for the phase function $\Phi(\mathbf{r},\theta,\varphi)$ and the evolution operator $\mathcal{F}(\mathbf{r},t)$:

$$\Phi(\tilde{G}_1\mathbf{r},\theta,\varphi)=\Phi(\mathbf{r},\theta,\varphi+\varphi_0), \tag{47a}$$

$$\mathcal{F}(\mathbf{r},t)=G_1\mathcal{F}(\tilde{G}_1\mathbf{r},t). \tag{47b}$$

The operator function $\mathcal{F}(\mathbf{r},t)$ defines both electric and magnetic vector fields $\mathbf{E}(\mathbf{r},t)$ and $\mathbf{B}(\mathbf{r},t)$ [Eq. (30)]. Their polarization states are dictated by the vector parameters $\mathbf{E}_0$ and $\mathbf{B}_0=\hat{\mathbf{k}}_0\times\mathbf{E}_0$.

The fields $\mathbf{W}_1$ and $\mathbf{W}_2$ can be conveniently described in terms of the cylindrical coordinates R, ψ, z, and the corresponding basis vectors $\mathbf{e}_R(\psi)$, $\mathbf{e}_A(\psi)$, and $\mathbf{e}_3$, related to $\mathbf{r}=x^1\mathbf{e}_1+x^2\mathbf{e}_2+x^3\mathbf{e}_3$ as follows:

$$\mathbf{r}(R,\psi,z)=R\mathbf{e}_R(\psi)+z\mathbf{e}_3, \tag{48a}$$

$$R=\sqrt{(x^1)^2+(x^2)^2}, \quad z=x^3. \tag{48b}$$

Since $\mathbf{r}(R,\psi,z)=G_1(\psi)\mathbf{r}(R,0,z)$, where $G_1(\psi)=\exp[\psi\mathbf{e}_3^{\times}]$ and $\mathbf{r}(R,0,z)=R\mathbf{e}_1+z\mathbf{e}_3$, the relation (47b) can be written in terms of the cylindrical coordinates as

$$\mathcal{F}(R,\psi,z,t)=G_1(\psi)\mathcal{F}(R,0,z,t). \tag{49}$$

As a consequence, one can relate field values in any two meridional planes by the operator of rotation G_1. In particular,

$$\mathbf{W}_i(R,\psi,z,t)=G_1(\psi)\mathbf{W}_i(R,0,z,t), \quad i=1,2. \tag{50}$$

Hence, to find the fields $\mathbf{W}_1$ and $\mathbf{W}_2$, it is sufficient to calculate their values in the plane ($\psi=0$) ($x^2=0$) and then to apply Eqs. (50). In this plane, the phase function $\Phi(\mathbf{r},\theta,\varphi)$ reduces to

$$\Phi(R',z',\theta,\varphi)=2\pi(R'\sin\theta\cos\varphi+z'\cos\theta-R_1\sin^2\theta-R_3\cos^2\theta), \tag{51}$$

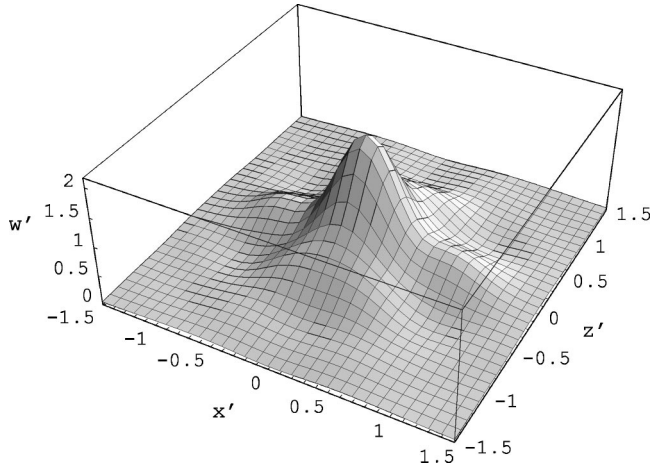

FIG. 3. Normalized energy density w' as a function of x' and z'; $y'=0$; $R_1=R_2=0.25$; $R_3=0.75$; $\varphi_1=\psi_1=\varphi$; $\varphi_2=\psi_2=\theta$; $\psi_3\equiv 0$; $\hat{\mathbf{k}}_0=\mathbf{e}_3$; $\mathbf{E}_0=\mathbf{e}_1$.

where $R'=R/\lambda$ and $z'=z/\lambda$. By making use of Eqs. (50) and (51), one can show that $\mathbf{W}_1$ and $\mathbf{W}_2$ satisfy the following orthogonality conditions:

$$\mathbf{e}_A(\psi)\cdot\mathbf{W}_1(R,\psi,z,t)=0, \tag{52a}$$

$$\mathbf{e}_R(\psi)\cdot\mathbf{W}_2(R,\psi,z,t)=0, \tag{52b}$$

$$\mathbf{e}_3\cdot\mathbf{W}_2(R,\psi,z,t)=0. \tag{52c}$$

If $R_1=R_2=R_3$, the fields $\mathbf{W}_1$ and $\mathbf{W}_2$ reduce to the earlier presented electromagnetic storms defined by the spherical harmonic Y_0^0, because the IPF becomes independent of both θ and φ [$\mathbf{r}_p'(\theta,\varphi)=R_1\hat{\mathbf{k}}(\theta,\varphi)$ and $\Phi_0(\theta,\varphi)\equiv 2\pi R_1$]. In this phase state, the storms have the vanishing time average energy flux at all points [23]. The condition $R_1=R_2\neq R_3$ results in a different phase state of these storms. The field remains highly localized (see Fig. 3), but now it has nonzero time average energy fluxes lying in the meridional planes, i.e., $S_2'(x',0,z')\equiv 0$ (see Figs. 4 and 5).

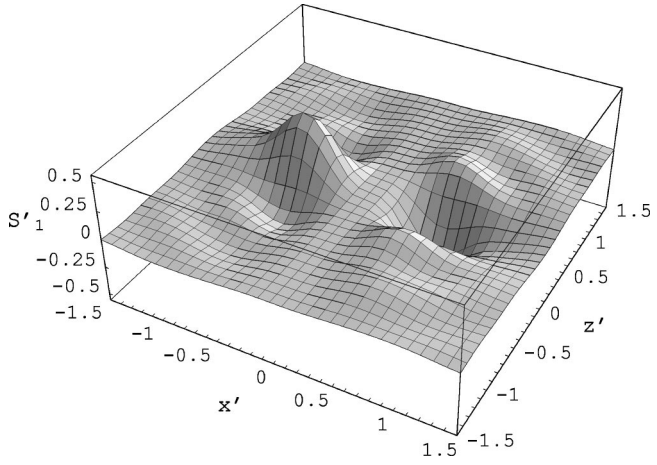

FIG. 4. Component S_1' of the normalized Poynting vector $\mathbf{S}'$ as a function of x' and z'; $y'=0$; the field parameters are the same as those in Fig. 3.

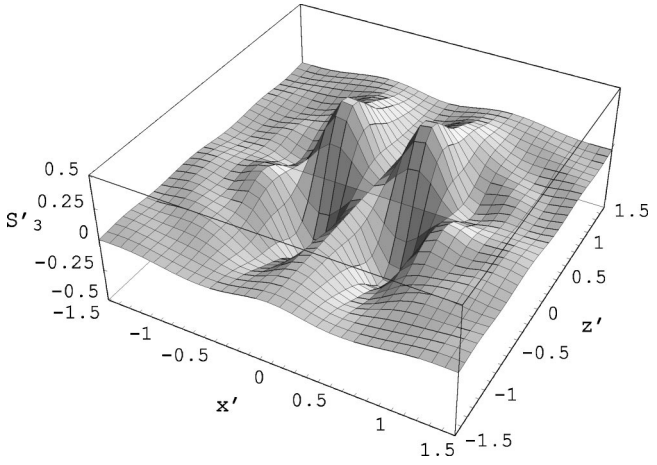

FIG. 5. Component S_3' of the normalized Poynting vector $\mathbf{S}'$ as a function of x' and z'; $y'=0$; the field parameters are the same as those in Fig. 3.

The time average energy density

$$w=\frac{1}{16\pi}(|\mathbf{E}|^2+|\mathbf{B}|^2) \tag{53}$$

and the cylindrical components of the time average Poynting vector

$$\mathbf{S}=\frac{c}{8\pi}\mathrm{Re}(\mathbf{E}\times\mathbf{B}^*) \tag{54}$$

are independent of the azimuthal angle ψ. Owing to Eqs. (44) these characteristics are the same for E_M and E_A fields. To illustrate the spatial distributions of energy density and energy fluxes, we use the dimensionless coordinates $x'=x^1/\lambda$, $y'=x^2/\lambda$, $z'=x^3/\lambda$, the normalized density $w'=w/w_0$, and the components $S_i'=\mathbf{e}_i\cdot\mathbf{S}'$ of the normalized Poynting vector $\mathbf{S}'=\mathbf{S}/S_0$, where $w_0=u_0^2/(8\pi)$ and $S_0=cw_0$.

It follows from Figs. 4 and 5 that both S_1' and S_3' are vanishing along the z' axis. The component S_1' reaches its peak in the plane $z'=0$ at $R'=|x'|\approx 0.6$. The radial component S_R' of $\mathbf{S}'$ is negative in the vicinity of this plane ($|z'|<0.3$), but it becomes positive at $|z'|>0.3$, ($S_R'=\pm S_1'$ for $x'=\pm R'$). The component S_3' reaches it maximum at $R'\approx 0.4$. The energy fluxes diverge from (converge to) the plane $z'=0$ at $R'<0.7$ ($R'>0.7$). It was shown in Ref. [23] that a change of the phase state of an electromagnetic storm or an orthonormal beam does not change the energy flux through any plane $z'=\mathrm{const}$. In the particular case under consideration, this general property remains valid. As a result, the density of energy fluxes divergent from the z plane is larger than the density of convergent fluxes, since the latter are distributed over a wider area.

B. Fields with $\psi_3\neq 0$

Let us now set $\mathbf{d}_0=\mathbf{e}_3$ and $\psi_3=\theta$. Let all other parameters be the same as before. In this case, $\mathbf{d}=\hat{\mathbf{k}}=\mathbf{e}_r$, i.e., the third

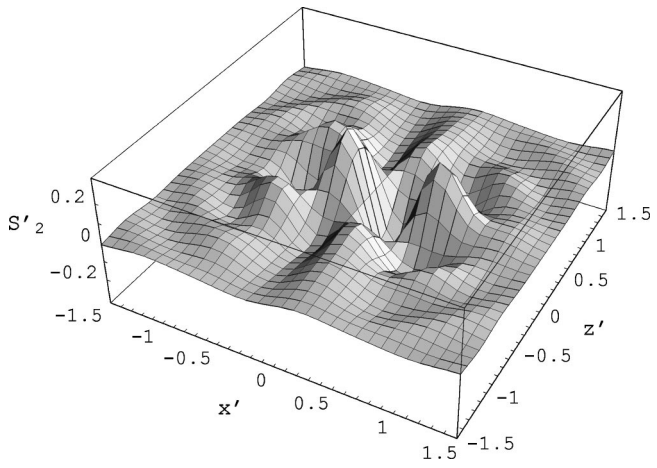

FIG. 6. Component S_2' of the normalized Poynting vector $\mathbf{S}'$ as a function of x' and z'; $y'=0$; $R_1=R_2=0.25$; $R_3=0.75$; $\varphi_1=\psi_1=\varphi$; $\varphi_2=\psi_2=\psi_3=\theta$; $\hat{\mathbf{k}}_0=\mathbf{d}_0=\mathbf{e}_3$; $\mathbf{E}_0=\mathbf{e}_1$.

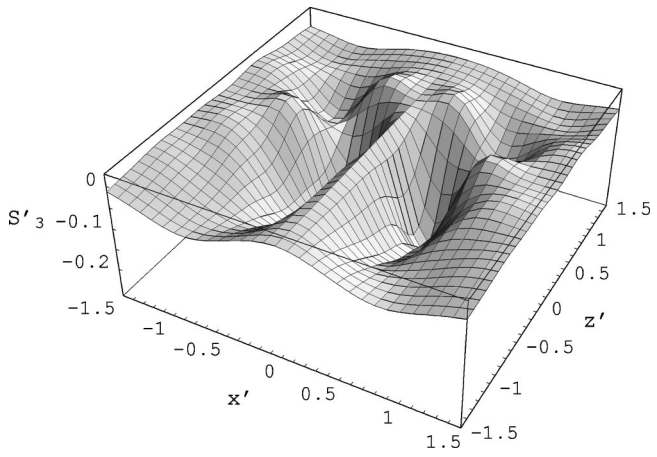

FIG. 7. Component S_3' of the normalized Poynting vector $\mathbf{S}'$ as a function of x' and z'; $y'=0$; $\mathbf{d}_0=(\mathbf{e}_1+\mathbf{e}_2)/2+\mathbf{e}_3/\sqrt{2}$; the other field parameters are the same as those in Fig. 6.

rotation [see Eqs. (28) and (33)] changes only the orientation of the eigenwave amplitudes **E** and **B**, but it does not change its direction of propagation. Accordingly, instead of the rotation operator $G(\theta,\varphi)$ [Eq. (41)], we obtain

$$G(\theta,\varphi)=(\mathbf{e}_M\cos\theta+\mathbf{e}_A\sin\theta)\otimes\mathbf{e}_1+(\mathbf{e}_A\cos\theta-\mathbf{e}_M\sin\theta)\otimes\mathbf{e}_2+\mathbf{e}_r\otimes\mathbf{e}_3. \tag{55}$$

Since the scalar coefficients in parentheses depend on θ, Eqs. (37) and (55) describe a new family of localized fields that cannot be represented as a linear superposition of the meridional $\mathbf{W}_1$ and the azimuthal $\mathbf{W}_2$ fields. Each member of this family is defined by a individual vector parameter $\mathbf{E}_0$. These fields still obey symmetry relations (47) and (49), but they cannot be treated as different phase states of the electromagnetic storms and whirls presented earlier.

The field with $\mathbf{E}_0=\mathbf{e}_1$ is slightly less localized and has smaller energy density w' ($\max w'=1.8$) and smaller components S_1' and S_3' ($\max S_1'=0.29$ and $\max S_3'=0.38$) than the field described in the previous section, but Figs. 3–5 still provide a rather good illustration of its properties in a qualitative sense. However, its major distinctive property is nonvanishing azimuthal energy fluxes (see Fig. 6). It is interesting that there are both clockwise and counterclockwise energy fluxes in the plane $z'=\text{const}$. Calculations show that, as before, $S_3'(R,\psi,0)\equiv 0$, i.e., there is no energy transport through the plane $z'=0$.

If $\mathbf{d}_0\neq\hat{\mathbf{k}}_0=\mathbf{e}_3$, the rotation through the angle $\psi_3=\theta$ around the unit vector $\mathbf{d}\neq\hat{\mathbf{k}}$ changes both the direction of propagation and the eigenwave amplitudes **E** and **B**. Let us set, for example, $\mathbf{d}_0=(\mathbf{e}_1+\mathbf{e}_2)/2+\mathbf{e}_3/\sqrt{2}$. This yields a field with nonzero energy flux through the plane $z'=0$ (see Fig. 7) and asymmetric (with respect to the plane $z'=0$) energy density distribution. For this field w' reaches its peak at $z'=0.45$.

V. FIELDS WITH TOROIDAL BM

In the case of a toroidal BM $\mathcal{B}=S_A^1\times S_B^1$, instead of $\mathcal{F}(\mathbf{r},t)$ [Eq. (37)], we obtain the evolution operator

$$\mathcal{F}(\mathbf{r},t)=\frac{u_0}{\pi}e^{-i\omega t}\int_0^{2\pi}d\varphi\int_0^{2\pi}e^{i\Phi(\mathbf{r},\theta,\varphi)}G(\theta,\varphi)\times(1+\rho\sin\theta)\,d\theta, \tag{56}$$

where $\rho=B/A\leqslant 1$, B is the radius of circles S_B^1, forming the toroidal surface ($\varphi=\text{const}, \theta\in[0,2\pi]$), provided that their centers are placed at a circle S_A^1 of radius A ($\pi AB=1$). We assume here that Eqs. (33), (38), and (40) remain valid.

In the above examples, the BM $\mathcal{B}=S^2$ (the unit sphere), the WVM $\mathcal{K}_3=S_k^2$ (the sphere of radius k), and ZPM $\mathcal{Z}_3$ (the ellipsoid) are two-dimensional differentiable manifolds with the same global topology. In other words, they are diffeomorphic to each other. The corresponding diffeomorphisms $\mathcal{B}\rightarrow\mathcal{K}_3$ and $\mathcal{B}\rightarrow\mathcal{Z}_3$ are given as $b\mapsto\mathbf{k}(b)=k\hat{\mathbf{k}}(b)$ and $b\mapsto\mathbf{r}_p=\lambda\mathbf{r}_p'$ for all $b\in\mathcal{B}=S^2$.

Let us now consider the surface $\mathcal{Z}_0$ given as

$$\mathbf{r}_p=\lambda\mathbf{r}_p'=\lambda[R_0(\mathbf{e}_1\cos\varphi_1+\mathbf{e}_2\sin\varphi_1)+\mathbf{e}_3R_3\cos\varphi_2], \tag{57a}$$

$$R_0=R_1+R_2\sin\varphi_2,\quad \varphi_1\in[0,2\pi],\quad \varphi_2\in[0,2\pi]. \tag{57b}$$

If R_1, R_2, and R_3 are nonvanishing, one can set the function $\mathbf{r}_p=\mathbf{r}_p(b)$ by some diffeomorphism $\mathcal{B}\rightarrow\mathcal{Z}_0$ of the toroidal BM $\mathcal{B}=S_A^1\times S_B^1$ onto $\mathcal{Z}_0$, using the entire $\mathcal{Z}_0$ as the ZPM ($\mathcal{Z}_3=\mathcal{Z}_0$). Alternatively, one can use some subset of $\mathcal{Z}_0$ as the ZPM ($\mathcal{Z}_3\subset\mathcal{Z}_0$) or assign zero values to some of the parameters R_i ($i=1,2,3$).

In the examples presented in this section, we assume that $\mathbf{d}_0=\mathbf{e}_1$. In this case, the rotation operator G [Eq. (33)] becomes

$$G=\mathbf{d}\otimes\mathbf{e}_1+\mathbf{g}_2\otimes\mathbf{e}_2+\mathbf{g}_3\otimes\mathbf{e}_3, \tag{58}$$

where

$$\mathbf{d}=\mathbf{e}_M(\psi_2,\psi_1)=\mathbf{e}_R(\psi_1)\cos\psi_2-\mathbf{e}_3\sin\psi_2, \tag{59a}$$

$$\mathbf{g}_2=\mathbf{e}_r(\psi_2,\psi_1)\sin\psi_3+\mathbf{e}_A(\psi_1)\cos\psi_3, \tag{59b}$$

$$\mathbf{g}_3=\mathbf{e}_r(\psi_2,\psi_1)\cos\psi_3-\mathbf{e}_A(\psi_1)\sin\psi_3. \qquad (59c)$$

A. Fields with a circular ZPM

Let us set the ZPM $\mathcal{Z}_3$ by Eq. (57), where $\varphi_1=\varphi$ and $R_2=R_3=0$. In this special case, the surface $\mathcal{Z}_0$ shrinks to the circle $\mathcal{Z}_3$ of radius R_1, lying in the plane $z'=0$. Any given point $\mathbf{r}_p(\varphi)$ of this circle is the image of the circle $S^1_B\subset\mathcal{B}$—the corresponding section of the toroidal BM.

Let us set the angles ψ_i as follows: $\psi_1=\varphi$, $\psi_2=2\varphi$, $\psi_3=\theta$. Substitution of Eqs. (57a) and (58) into Eqs. (38) and (56) yields the evolution operator $\mathcal{F}(\mathbf{r},t)$ that describes a family of fields with the circular ZPM $\mathcal{Z}_3$. The members of this family have different WVMs $\mathcal{K}_3$ and PMs $\mathcal{P}_3$, specified by the values of $\hat{\mathbf{k}}_0$ and $\mathbf{E}_0$ [see Eqs. (28)]. Their common feature is that $\mathbf{r}_p$ and $\mathbf{d}$ depend only on φ. As a result, any point $\mathbf{r}_p(\varphi)$ of the zero phase circle $\mathcal{Z}_3$ corresponds to a subset of partial eigenwaves with triads $[\hat{\mathbf{k}}_0(\theta,\varphi),\mathbf{E}(\theta,\varphi),\mathbf{B}(\theta,\varphi)]$, related to each other by rotations around $\mathbf{d}(\varphi)$ ($\theta\in[0,2\pi]$, $\varphi=\text{const}$).

In particular, if $\mathbf{k}_0=\mathbf{e}_3$, $\mathbf{E}_0=\mathbf{e}_1$, and $\mathbf{B}_0=\mathbf{e}_2$, the WVM is defined by the function $\mathbf{k}(\theta,\varphi)=k\mathbf{g}_3(\theta,\varphi)$. In terms of the electric and magnetic fields, the corresponding PM is defined by the functions $\mathbf{E}(\theta,\varphi)=\mathbf{d}(\varphi)$ and $\mathbf{B}(\theta,\varphi)=\mathbf{g}_2(\theta,\varphi)$, respectively. Upon integrating fields of partial eigenwaves over $\theta\in[0,2\pi]$ we obtain an infinitesimal electromagnetic wave (wavelet)—the superposition of eigenwaves corresponding to an arbitrary given $\varphi=\varphi_0$. The electric field of this wavelet is linearly polarized along $\mathbf{d}(\varphi_0)$ at any point $\mathbf{r}$. By the construction of $\mathcal{F}(\mathbf{r},t)$, the initial phases of all eigenwaves forming the wavelet vanish at the point $\mathbf{r}_0=\mathbf{r}_p(\varphi_0)\in\mathcal{Z}_3$. At this point, the electric field of the wavelet reaches its absolute maximum independent of ρ, whereas the magnetic field takes a value depending on ρ. Upon integrating the electric field of wavelets over $\varphi\in[0,2\pi]$ we obtain the total field $\mathbf{E}(\mathbf{r},t)$ constructed so that a major contribution to the field value $\mathbf{E}(\mathbf{r}_0,t)$ at any point $\mathbf{r}_0=\mathbf{r}_p(\varphi_0)$ of the circle $\mathcal{Z}_3$ yield wavelets with parameters φ lying in a neighborhood of φ_0. Since other wavelets differ widely in polarization, magnitude, and phase at this point, they suppress each other and thus decrease their contribution to the total field in this neighborhood. By the same reasoning the magnetic field in the neighborhood of the circle $\mathcal{Z}_3$ is smaller than the electric field. Figures 8–10 illustrate properties of the described localized fields for two different values of parameter ρ. In Fig. 9 and thereafter, the normalized instantaneous electric field is defined as $\mathbf{E}'=\mathrm{Re}\,\mathbf{E}/E_0$, where $E_0=u_0/\sqrt{4\pi}$.

B. Fields with two-dimensional $\mathcal{Z}_3$

For the fields under consideration, every phase state is described by a subset $\mathcal{Z}_3\subseteq\mathcal{Z}_0$, parametrized by the points of the BM $\mathcal{B}$. In the preceding section, we considered some fields with one-dimensional (circular) $\mathcal{Z}_3$, where every point $\mathbf{r}_p\in\mathcal{Z}_3$ is the image of a subset of $\mathcal{B}$ (circle $\varphi=\text{const}$). Here we present three examples of fields with two-dimensional $\mathcal{Z}_3$ defined by an injective (one-one) mapping of $\mathcal{B}$ onto $\mathcal{Z}_0$. Different mappings $\mathbf{r}_p=\mathbf{r}_p(b)$ of $\mathcal{B}$ onto the same surface $\mathcal{Z}_0$ give different phase states (parametrizations $\mathcal{Z}_3$ of $\mathcal{Z}_0$).

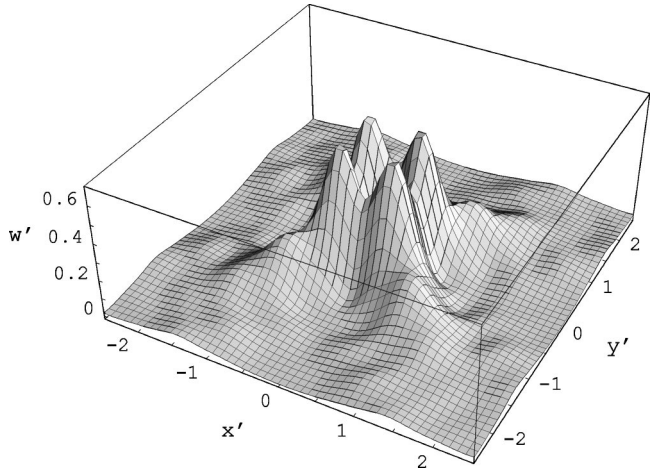

FIG. 8. Normalized energy density w' as a function of x' and y'; $z'=0$; $\rho=0.05$; $R_1=0.5$; $R_2=R_3=0$; $\varphi_1=\psi_1=\varphi$, $\psi_2=2\varphi$, $\psi_3=\theta$; $\hat{\mathbf{k}}_0=\mathbf{e}_3$; $\mathbf{d}_0=\mathbf{E}_0=\mathbf{e}_1$.

These mappings can be given in terms of local coordinate (θ,φ) on $\mathcal{B}$ and (φ_1,φ_2) on $\mathcal{Z}_0$, but the corresponding phase state is independent of the choice of the coordinates systems. Similarly, all other properties of the field are defined by the coordinate-free mappings $\mathcal{B}\to\mathcal{K}_3$, $\mathcal{B}\to\mathcal{P}_3$, and $u=u(b)$.

In all three examples, we set $R_1=0.75$, $R_2=R_3=0.25$, $\hat{\mathbf{k}}_0=\mathbf{e}_3$, and $\mathbf{d}_0=\mathbf{E}_0=\mathbf{e}_1$, i.e., the operator of rotation is given by Eqs. (58). Let us first obtain an axially symmetric E_M field with $\mathcal{Z}_3$ diffeomorphic to $\mathcal{B}$. To this end, we set $\varphi_1=\psi_1=\varphi$, $\varphi_2=\psi_2=\theta$, and $\psi_3\equiv 0$. In this case, the two sets of orthogonal coordinate curves on $\mathcal{B}$ (circles $\varphi=\text{const}$ and $\theta=\text{const}$) are one-one mapped onto the similar sets of coordinate circles on $\mathcal{Z}_0$. However, the mappings $\mathbf{k}(\theta,\varphi)=k\mathbf{e}_r(\theta,\varphi)$, $\mathbf{E}(\theta,\varphi)=\mathbf{e}_M(\theta,\varphi)$, $\mathbf{B}(\theta,\varphi)=\mathbf{e}_A(\varphi)$, defining the WVM $\mathcal{K}_3$ and the PM $\mathcal{P}_3$, are not injective.

Figure 11 illustrates the total energy density $w'=w'_e+w'_m$ of the obtained localized field. Owing to the built-in symmetry, the electric field density w'_e peaks at the z axis,

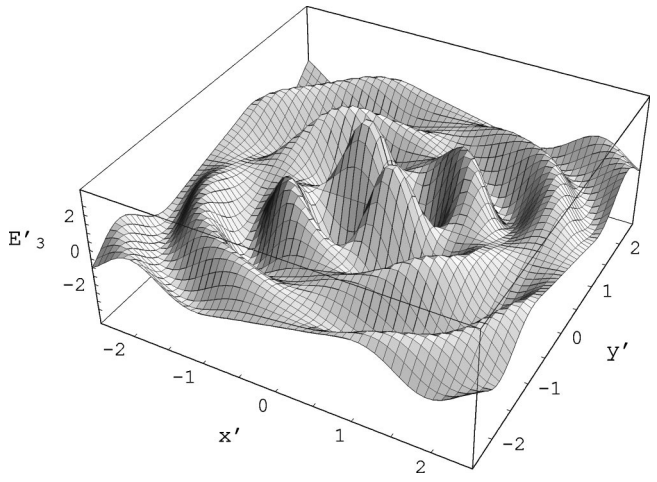

FIG. 9. Component E'_3 of the normalized instantaneous electric field $\mathbf{E}'$ as a function of x' and y'; $z'=0$; $t=0$; the field parameters are the same as those in Fig. 8.

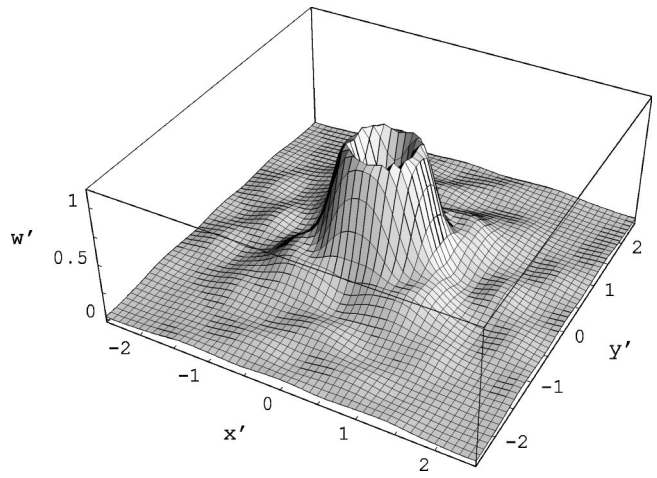

FIG. 10. Normalized energy density w' as a function of x' and y'; $z'=0$; $\rho=1$; the other field parameters are the same as those in Figs. 8 and 9.

whereas the magnetic field density w'_m and the time average Poynting vector **S** are vanishing at this axis. The azimuthal components of **S** and **E**, as well as the z component of **B**, are everywhere zero.

Let us now change the phase state of the above field by defining the parametrization $\mathcal{Z}_3$ of $\mathcal{Z}_0$ as

$$\varphi_1=2\varphi, \quad \varphi_2=0.5\theta+\varphi, \tag{60}$$

where $0\leqslant\varphi<2\pi$, and $0\leqslant\theta<2\pi$. In this case, $\mathcal{K}_3$ and $\mathcal{P}_3$ remain as before, but the mapping $\mathcal{B}\rightarrow\mathcal{Z}_0$ is not continuous at the circle $\theta=0$ on $\mathcal{B}$, since every coordinate circle $\varphi=$const on $\mathcal{B}$ is mapped onto a semicircle on $\mathcal{Z}_0$. Every coordinate circle $\theta=$const on $\mathcal{B}$ is mapped onto a closed curve that makes two complete revolutions around the hole of $\mathcal{Z}_0$ and each time intersects the plane $z'=0$. The described phase change breaks the initial axial symmetry and produces a well-localized field with the domain of localization shifted in the x' direction (see Fig. 12) and rather complicated structure of energy fluxes.

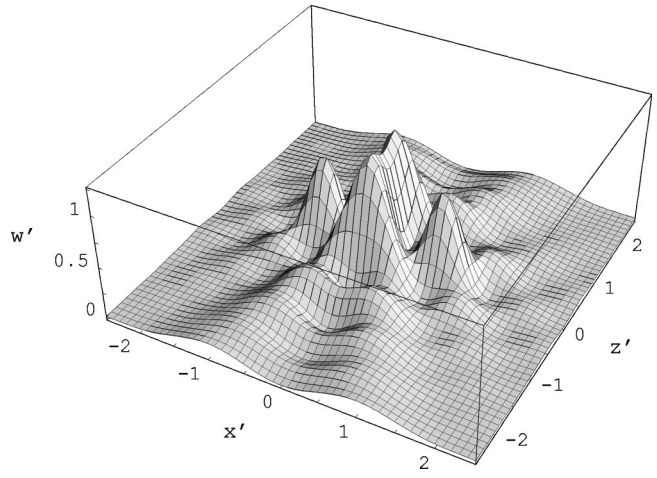

FIG. 11. Normalized energy density w' as a function of x' and z'; $y'=0$; $\rho=0.5$; $R_1=0.75$; $R_2=R_3=0.25$; $\varphi_1=\psi_1=\varphi$; $\varphi_2=\psi_2=\theta$; $\psi_3\equiv 0$; $\hat{\mathbf{k}}_0=\mathbf{e}_3$; $\mathbf{d}_0=\mathbf{E}_0=\mathbf{e}_1$.

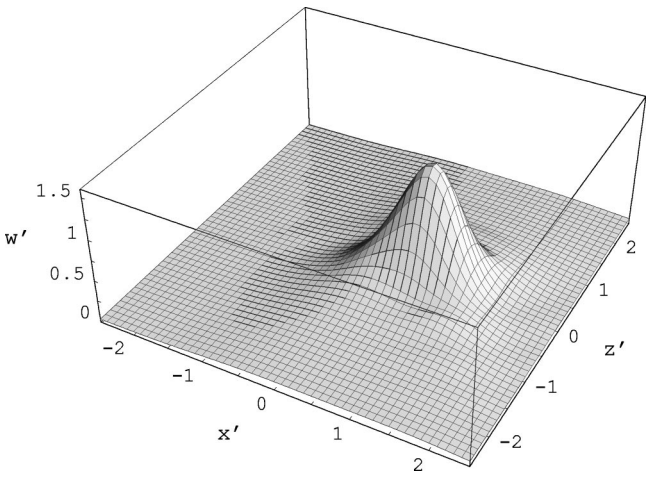

FIG. 12. Normalized energy density w' as a function of x' and z'; $y'=0$; $\rho=0.5$; $R_1=0.75$; $R_2=R_3=0.25$; $\varphi_1=2\varphi$; $\varphi_2=0.5\theta+\varphi$; $\psi_1=\varphi$; $\psi_2=\theta$; $\psi_3\equiv 0$; $\hat{\mathbf{k}}_0=\mathbf{e}_3$; $\mathbf{d}_0=\mathbf{E}_0=\mathbf{e}_1$.

As the third example, let us construct an axially symmetric field with nonvanishing azimuthal energy fluxes. To this end, it is sufficient to set the parameters as follows: $\varphi_1=\psi_1=\varphi$, $\varphi_2=\psi_2=\psi_3=\theta$. In this case, $\mathcal{Z}_3$ remains the same as in the first example, but both $\mathcal{K}_3$ and $\mathcal{P}_3$ are different, since the condition $\psi_3\equiv 0$ is replaced by $\psi_3=\theta$. Figures 13–16 illustrate the properties of the obtained field. To reverse the direction of the azimuthal fluxes, it is necessary to set $\psi_3=-\theta$. The structure of the azimuthal fluxes can be modified by changing the BM parameter ρ. The other two cylindrical components of **S** are scarcely affected by a change of this parameter.

VI. COMPLEX FIELD STRUCTURES

A. Field gratings

The presented electromagnetic fields have a very small (about several wavelengths) core region with maximum intensity of field oscillations and unique space distributions of

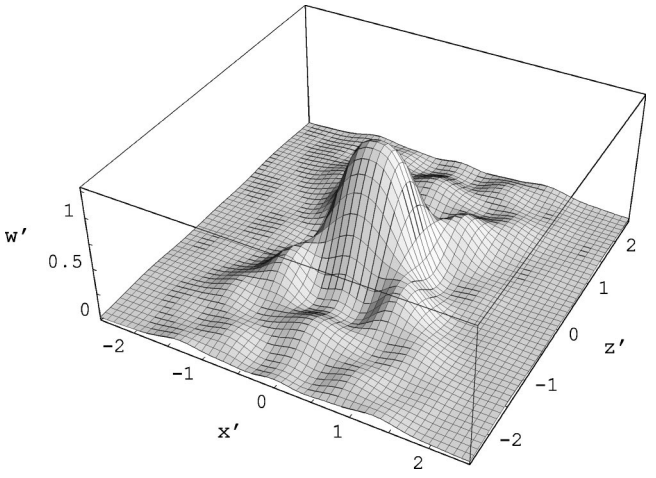

FIG. 13. Normalized energy density w' as a function of x' and z'; $y'=0$; $\rho=0.5$; $R_1=0.75$; $R_2=R_3=0.25$; $\varphi_1=\psi_1=\varphi$, $\varphi_2=\psi_2=\psi_3=\theta$; $\hat{\mathbf{k}}_0=\mathbf{e}_3$; $\mathbf{d}_0=\mathbf{E}_0=\mathbf{e}_1$.

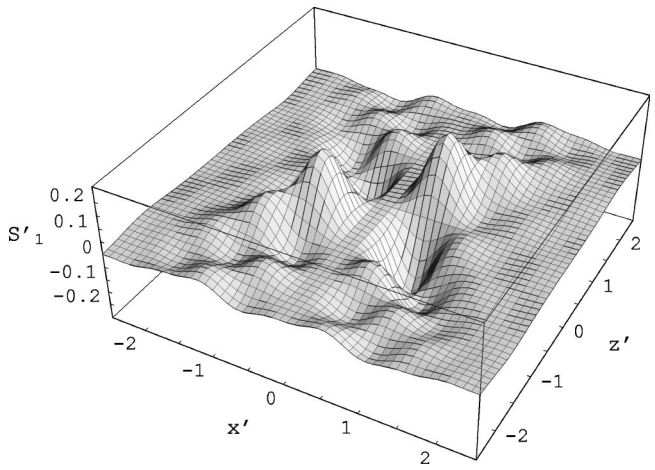

FIG. 14. Component S_1' of the normalized Poynting vector $\mathbf{S}'$ as a function of x' and z'; $y'=0$; the field parameters are the same as those in Fig. 13.

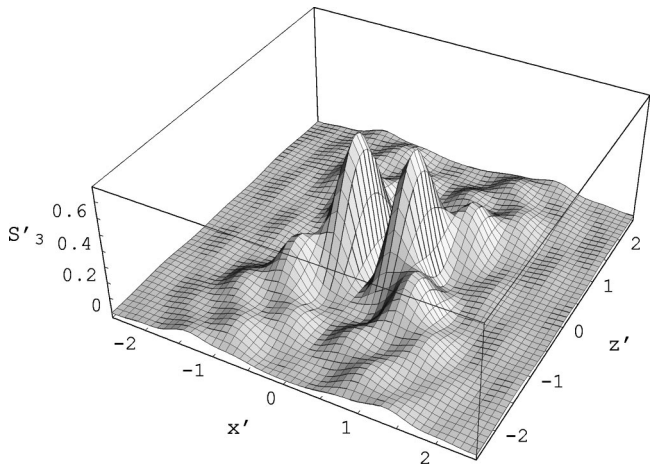

FIG. 16. Component S_3' of the normalized Poynting vector $\mathbf{S}'$ as a function of x' and z'; $y'=0$; the field parameters are the same as those in Fig. 13.

polarization states, energy densities, and energy fluxes. Outside the core, the intensity of oscillations rapidly decreases in all directions. The three-dimensional localization makes it possible to use these fields as structural elements to form various complex electromagnetic fields.

By way of illustration, let us consider a field defined as

$$\mathbf{W}'(\mathbf{r},t)=\sum_{n=M_1}^{N_1}\sum_{m=M_2}^{N_2}\sum_{l=M_3}^{N_3}\mathbf{W}(\mathbf{r}-\mathbf{a}_{nml},t-\tau_{nml}), \tag{61a}$$

$$\mathbf{a}_{nml}=n\mathbf{a}_1+m\mathbf{a}_2+l\mathbf{a}_3, \tag{61b}$$

$$\tau_{nml}=n\tau_1+m\tau_2+l\tau_3, \tag{61c}$$

where $\mathbf{W}(\mathbf{r},t)$ is set by Eq. (12), $\mathbf{a}_j$ and τ_j are some given spatial and temporal shifts.

On the one hand, this field can be treated as a different state of $\mathbf{W}(\mathbf{r},t)$, obtained by the magnitude function transformation $u(b)\mapsto u(b)|h(b)|$ and the phase transformation $\Phi(\mathbf{r},t,b)\mapsto\Phi(\mathbf{r},t,b)+\Delta\Phi(b)$. Here, $|h(b)|$ and $\Delta\Phi(b)$ are defined as

$$h(b)\equiv|h(b)|e^{\Delta\Phi(b)}=h_1(b)h_2(b)h_3(b), \tag{62}$$

where

$$h_j(b)=\sum_{m=M_j}^{N_j}e^{im\Phi_j(b)}=\frac{\exp[iM_j\Phi_j(b)]-\exp[i(N_j+1)\Phi_j(b)]}{1-\exp[i\Phi_j(b)]}, \tag{63}$$

$$\Phi_j(b)=\omega(b)\tau_j-\mathbf{k}(b)\cdot\mathbf{a}_j. \tag{64}$$

However, these fields have the same WVM $\mathcal{K}_3$ and the same PM $\mathcal{P}_3$.

On the other hand, the translated fields $\mathbf{W}(\mathbf{r}-\mathbf{a}_{nml},t-\tau_{nml})$ form a family of wavelets with $\mathbf{W}(\mathbf{r},t)$ as the mother wavelet. Hence, if $\mathbf{W}$ is one of the foregoing localized fields, and lengths of the shift vectors $\mathbf{a}_j$ $(j=1,2,3)$ are sufficiently large, the field $\mathbf{W}'$ will constitute a field grating. Figures 17 and 18 depict component E_3' of the normalized instantaneous electric field $\mathbf{E}'$ of the three-dimensional (cubic) grating at two different instants $t=0$ and $t'=0.25$ $[t'=t/T=\omega t/(2\pi)]$, respectively. The grating is composed of 27 E_M storms $\mathbf{E}_j^s$ $(j=s=0)$, whose properties are described in some details in Ref. [23]. In the next section, we consider the influence of this grating on relativistic electrons.

The great diversity of the presented localized fields with different geometries of core regions provides a great scope for combining them, as constructive elements, into various one-, two-, or three-dimensional gratings and other complex geometrical structures, where each element has only reasonably small deviations from its initial form.

Moreover, the prior investigation of a single localized field permits us to use copies of this field with small spatial and time shifts in designing complex electromagnetic fields.

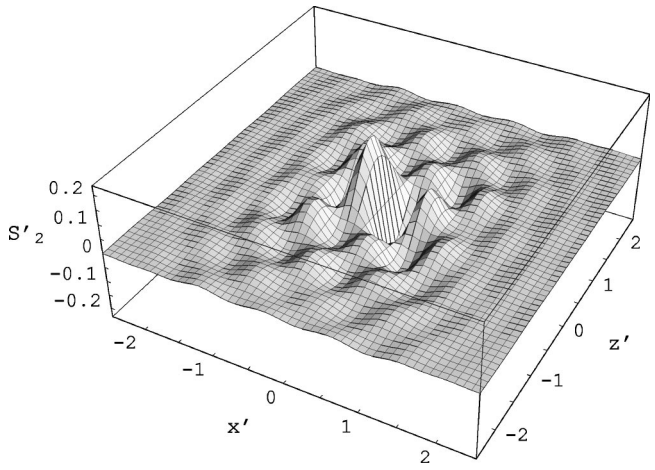

FIG. 15. Component S_2' of the normalized Poynting vector $\mathbf{S}'$ as a function of x' and z'; $y'=0$; the field parameters are the same as those in Fig. 13.

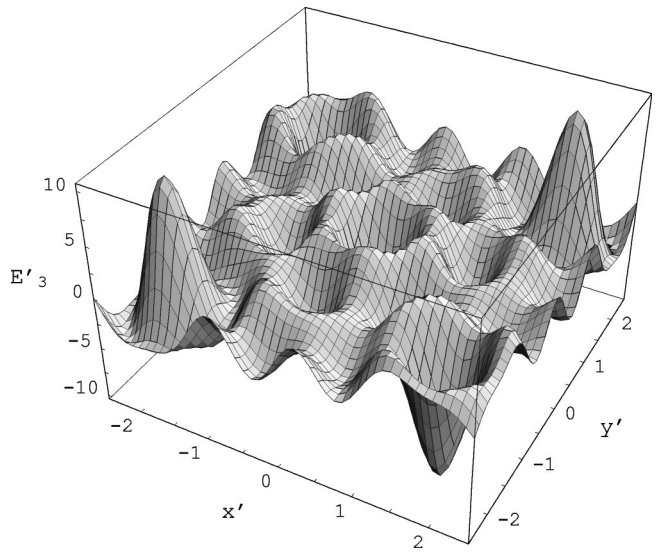

FIG. 17. Component E_3' of the normalized instantaneous electric field $\mathbf{E}'$ of the cubic grating composed of 27 storms E_0^0 as a function of x' and y'; $z'=0$; $M_1=M_2=M_3=-1$; $N_1=N_2=N_3=1$; $\mathbf{a}_i'=\mathbf{a}_i/\lambda=1.75\mathbf{e}_i$, $\tau_i'=\omega\tau_i/(2\pi)=1.75$ $(i=1,2,3)$; $t=0$.

Designing localized electromagnetic fields to control motion and state of charged and neutral particles (atoms and molecules) is a possible application of the presented techniques. In the following section, we illustrate this on an example of relativistic charged particles.

B. Charged particles in localized fields

Let m_0 and e be the rest mass and the charge of a relativistic particle moving in an electromagnetic field F. Taking into account Eq. (3), the relativistic equation of motion can be written as [33]

$$m_0 c\frac{d\mathbf{u}}{ds}=\mathbf{Q}, \tag{65}$$

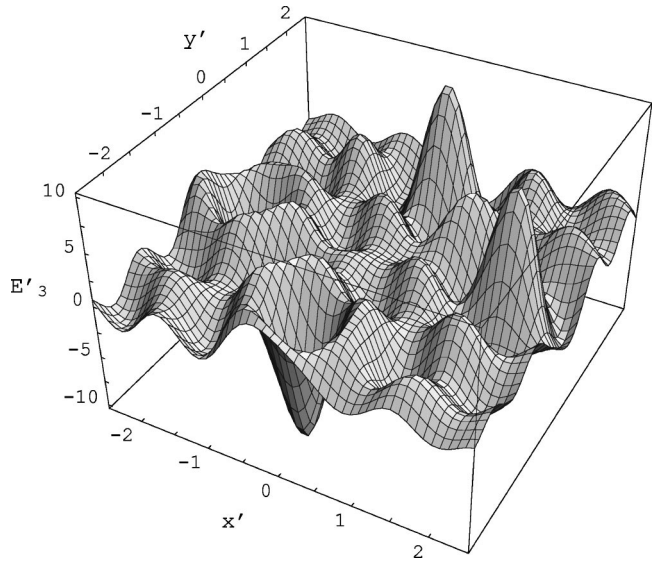

FIG. 18. Component E_3' at $t'=0.25$; the other field parameters are the same as those in Fig. 17.

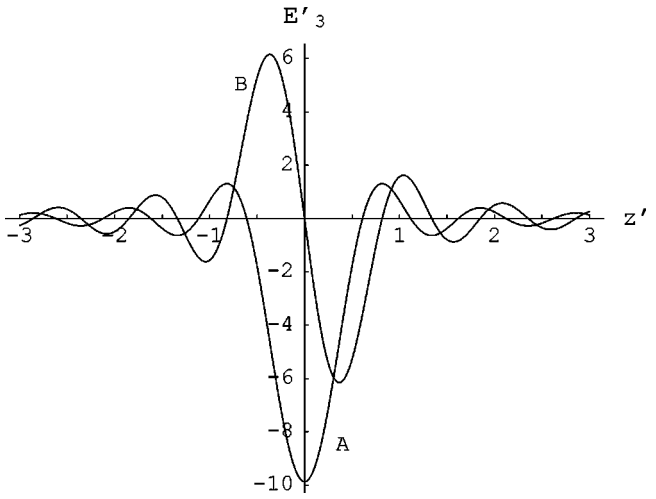

FIG. 19. Component E_3' of the normalized instantaneous electric field $\mathbf{E}'$ of E_M storms as a function of z'; $x'=y'=0$; (A) $j=s=0$, $t=0$; (B) $j=1$, $s=0$, $t'=0.25$.

where

$$Q^i=\frac{e}{c}F^{ik}u_k+\frac{2e^3}{3m_0c^3}\frac{\partial F^{ik}}{\partial x^l}u^l u_k+\frac{2e^4}{3m_0^2c^5}\times[F^{ik}F_{kl}u^l+(u_mF^{mk})(F_{kl}u^l)u^i], \tag{66}$$

$$\mathbf{u}=\frac{d\mathbf{x}}{ds},\quad \gamma=(1-\beta^2)^{-1/2}, \tag{67}$$

$ds=cdt/\gamma$, $\boldsymbol{\beta}=\mathbf{v}/c$, $\mathbf{v}$ is the velocity of the particle, and summation over repeated indices is carried out from 1 to 4. The tensor F of a field grating can be readily found from Eq. (1), provided that $\mathbf{E}$ and $\mathbf{B}$ are calculated as described above. Hence, if the initial velocity and the initial position of the charged particle are given, one can investigate its motion by using point-by-point integration of Eqs. (65)–(67).

Let us consider two examples. In both cases, as the mother wavelet, we use the electromagnetic E_M storm $\mathbf{E}_0^0$ [Eq. (15)]. The E_M storm $\mathbf{E}_j^0$, defined by the zonal spherical harmonic Y_j^0, is a localized field with the meridional orientation of the electric field $\mathbf{E}$ and azimuthal orientation of the magnetic field $\mathbf{B}$ [23]. At any point of the z axis, $\mathbf{E}$ is directed along this axis, and $\mathbf{B}=0$. Figure 19 shows the only nonzero component E_3' of the instantaneous electric field of $\mathbf{E}_0^0$ and $\mathbf{E}_1^0$ storms at the z axis. Although both fields are highly localized, a relativistic charged particle (electron, in the following illustrations), moving through the core region ($|z'|<1$) along the z axis, is alternately subjected to acceleration and deceleration. However, one can construct a complex localized field with the same axial symmetry and the extended domain of acceleration (deceleration). To this end, it is sufficient to combine a number of $\mathbf{E}_0^0$ storms into a one-dimensional grating with small spatial and temporal shifts (see Fig. 20). In this case, the particle can be continuously accelerated (decelerated) during several periods of oscillation $T=2\pi/\omega$. The initial coordinates $x_0'=x'(t_0')$, $y_0'=y'(t_0')$,

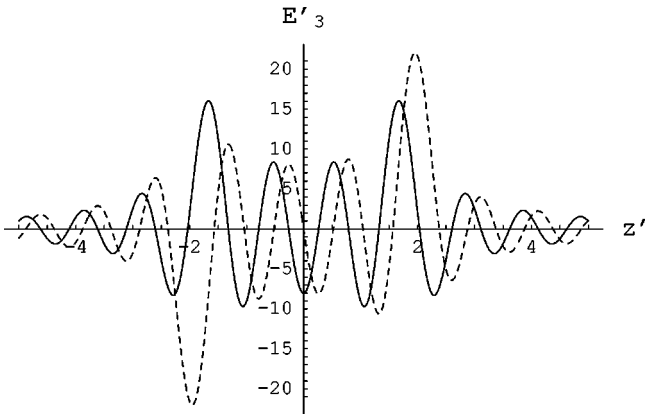

FIG. 20. Component E_3' of the normalized instantaneous electric field $\mathbf{E}'$ of a complex field composed of 31 E_M storms $\mathbf{E}_0^0$ as a function of z' at $t=0$ (solid curve) and $t'=0.25$ (dashed-line curve); $x'=y'=0$; $M_1=N_1=M_2=N_2=0$; $M_3=-15$; $N_3=15$; $\mathbf{a}_3'=0.125\mathbf{e}_3$; $\tau_3'=0.125$.

$z_0'=z'(t_0')$, and the initial time $t_0'=t_0/T$ specify the dependence of the relativistic factor γ on z' (see Figs. 21–23). As a consequence of the built-in spatial and temporal shifts ($\tau_3'>0$) of the $\mathbf{E}_0^0$ storms forming the complex field, the particles, moving in the positive and the negative directions, have quite different dependences $\gamma=\gamma(z')$ (see Fig. 23).

The above cubic field grating with large spatial and temporal shifts (see Figs. 17 and 18) affects the particle motion in a different three-stage manner. Figures 24 and 25 illustrate the dependence of γ on z' for six electrons that have the same initial velocity $\beta_0=0.9997\mathbf{e}_3$ at $t_0'=-5$, but different initial coordinates x_0' and y_0' at the plane $z_0'=-5$.

VII. CONCLUSION

In this paper, an important approach to characterizing and designing localized electromagnetic fields, based on the use of differentiable manifolds, differentiable mappings, and the group of rotation, is presented. The beam manifold $\mathcal{B}$, the wave-vector manifold $\mathcal{K}$, the polarization manifold $\mathcal{P}$, the zero phase manifold $\mathcal{Z}$, and the magnitude function u are the key elements of the Lorentz covariant description. Every localized field under consideration is characterized by the differentiable mappings $\mathcal{B}\to\mathcal{K}$, $\mathcal{B}\to\mathcal{P}$, $\mathcal{B}\to\mathcal{Z}$, and $\mathcal{B}\to R$, given as $\mathbf{K}=\mathbf{K}(b)$, $\mathbf{f}=\mathbf{f}(b)$, $\mathbf{x}_p=\mathbf{x}_p(b)$, and $u=u(b)$. They specify wave vectors, polarizations, initial phases, and magnitudes of eigenwaves constituting the field. If the field is time harmonic in a frame L, one can characterize it by the corresponding sections $\mathcal{K}_3$, $\mathcal{P}_3$, and $\mathcal{Z}_3$ of $\mathcal{K}$, $\mathcal{P}$, and $\mathcal{Z}$.

By way of illustration, families of exact time-harmonic solutions to Maxwell's equations in the source-free space—fields defined by the rotation group—are presented. These families describe localized fields with two-dimensional beam manifolds that are topologically distinct (spherical and toroidal BMs). For every field, both wave vectors and normalized amplitudes of partial eigenwaves are set by the same rotation operator function.

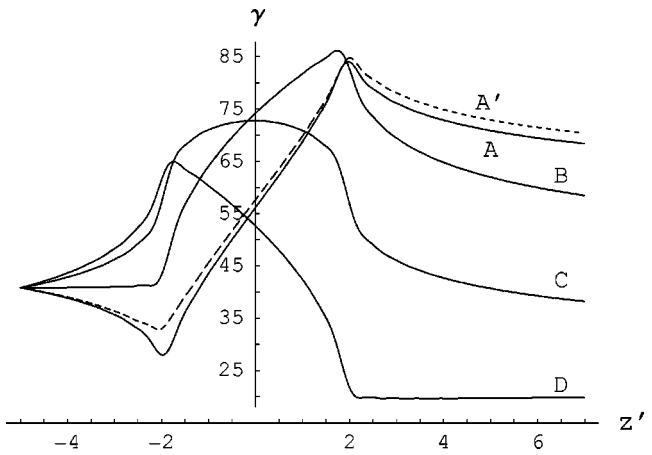

FIG. 21. Relativistic factor γ of electron moving in the complex field as a function of z'; $y_0'=0$; (A') $t_0'=-5$; $x_0'=0.25$; (A) $t_0'=-5$; (B) $t_0'=-4.875$; (C) $t_0'=-4.75$; (D) $t_0'=-4.625$; $x_0'=0$ for curves A, B, C, and D; $\beta_0=0.9997$; $\lambda=10.6$ μm; $E_3=-5.9\times10^9$ V/cm at $t=0$ and $z=0$; the other field parameters are the same as those in Fig. 20.

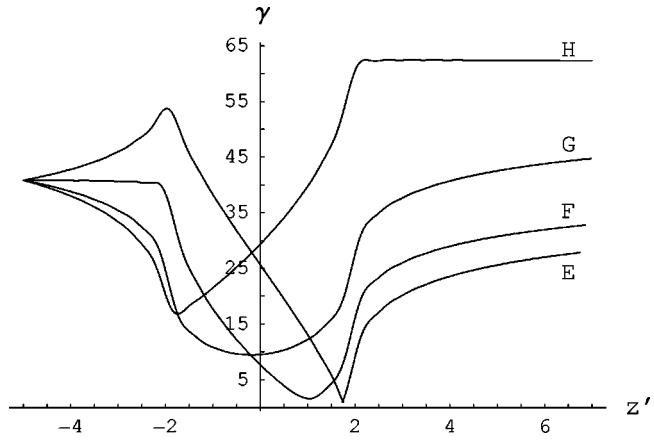

FIG. 22. Relativistic factor γ of electron moving in the complex field as a function of z'; $x_0'=y_0'=0$; (E) $t_0'=-4.5$; (F) $t_0'=-4.375$; (G) $t_0'=-4.25$; (H) $t_0'=-4.125$; the field parameters are the same as those in Figs. 20 and 21.

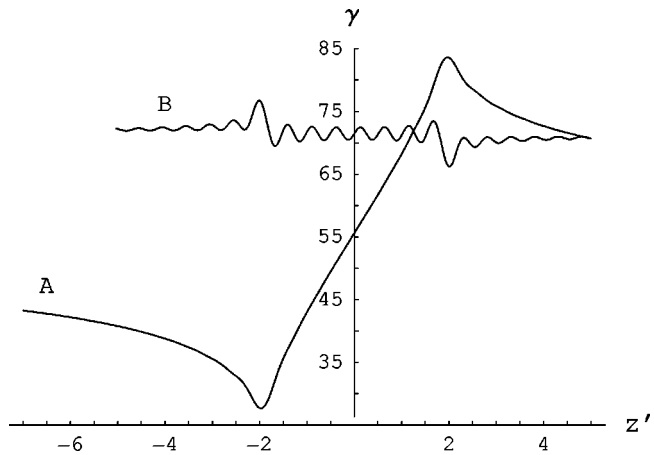

FIG. 23. Relativistic factor γ of electron moving in (A) the positive z direction; (B) the negative z direction; the field parameters are the same as those in Figs. 20 and 21.

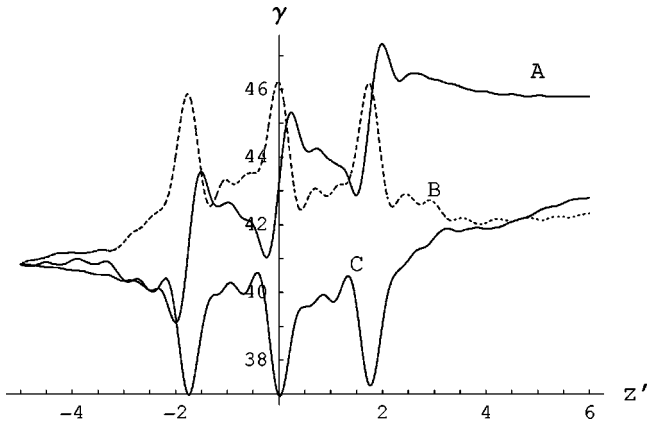

FIG. 24. Relativistic factor γ of electron moving in the three-dimensional field grating as a function of z'; $t_0'=-5$; $z_0'=-5$; $y_0'=0$; $\beta_0=0.9997$; (*A*) $x_0'=0$; (*B*) $x_0'=1.75$; (*C*) $x_0'=-1.75$; $\lambda=10.6$ μm; $E_3=-7.16\times10^9$ V/cm at $t=0$ and $z=0$; the other field parameters are the same as those in Fig. 17.

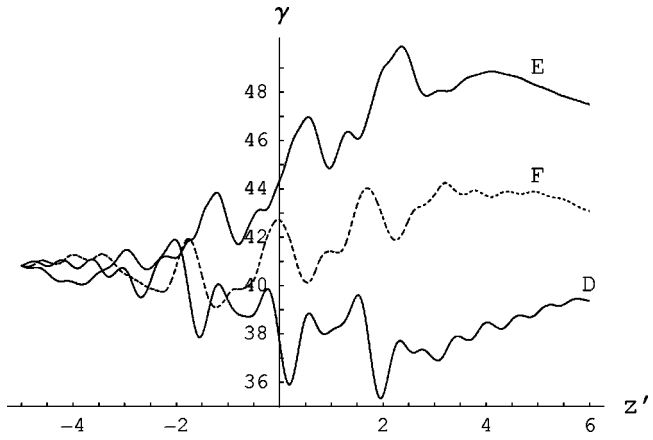

FIG. 25. Relativistic factor γ of electron moving in the three-dimensional field grating as a function of z'; (*D*) $x_0'=y_0'=1.75$; (*E*) $x_0'=y_0'=0.25$; (*F*) $x_0'=y_0'=0.875$; the other parameters are the same as those in Figs. 17 and 24.

It is shown that the proposed approach provides a broad spectrum of tools to design localized fields, i.e., to build-in symmetry properties of oscillating electric and magnetic fields, to govern the distributions of their energy densities (both size and form of localization domains), and to set the structure of time-average energy fluxes.

Localized fields of one or more types can be combined as constructive elements to obtain a complex field structure with desirable properties, such as one-, two-, or three-dimensional field gratings.

The proposed approach can be used in designing localized electromagnetic fields to govern motion and state of charged and neutral particles. In particular, the results described in the preceding section give promise that the field gratings and other complex localized electromagnetic fields may be applied in free-electron lasers and electromagnetic propulsion devices (ion thrusters). In both cases, the localization of energy in small domains of wavelength size is an advantageous property. It results in strong electric and magnetic fields in their (typically different) domains of localization. Besides it makes possible to construct a three-dimensional field grating with a multitude of parallel many-stage acceleration channels. When employing this grating as an ion thruster, electron and positive ion packets can move along either the same channels with the time shift $nT/2$ (n is an odd integer) or different parallel channels. In the latter case, the phase shifts of localized fields along the corresponding channels can be set differently to optimize acceleration of both electrons and ions. With these applications in mind, it is important to remember that localized electromagnetic fields can also be designed to counteract Coulomb repulsing of charged particles and, thus, to catalyze the forming of localized particle packets [11,18].

[1] J.N. Brittingham, J. Appl. Phys. **54**, 1179 (1983).
[2] A. Sezginer, J. Appl. Phys. **57**, 678 (1985).
[3] R.W. Ziolkowski, J. Math. Phys. **26**, 861 (1985).
[4] T.T. Wu, J. Appl. Phys. **57**, 2370 (1985).
[5] J. Durnin, J. Opt. Soc. Am. A **4**, 651 (1987).
[6] J. Durnin, J.J. Miceli, and J.H. Eberly, Phys. Rev. Lett. **58**, 1499 (1987).
[7] R.W. Ziolkowski, D.K. Lewis, and B.D. Cook, Phys. Rev. Lett. **62**, 147 (1989).
[8] R.W. Ziolkowski, Phys. Rev. A **39**, 2005 (1989).
[9] A.M. Shaarawi, I.M. Besieris, and R.W. Ziolkowski, J. Appl. Phys. **65**, 805 (1989).
[10] R.W. Ziolkowski and D.K. Lewis, J. Appl. Phys. **68**, 6083 (1990).
[11] R.W. Ziolkowski and M.K. Tippett, Phys. Rev. A **43**, 3066 (1991).
[12] R.W. Ziolkowski, Phys. Rev. A **44**, 3960 (1991).
[13] P.L. Overfelt, Phys. Rev. A **44**, 3941 (1991).
[14] R. Donnelly and R.W. Ziolkowski, Proc. R. Soc. London, Ser. A **437**, 673 (1992).
[15] R.Donnelly and R.W. Ziolkowski, Proc. R. Soc. London, Ser. A **440**, 541 (1993).
[16] R.W. Ziolkowski, I.M. Besieris, and A.M. Shaarawi, J. Opt. Soc. Am. A **10**, 75 (1993).
[17] A.M. Shaarawi, R.W. Ziolkowski, and I.M. Besieris, J. Math. Phys. **36**, 5565 (1995).
[18] R.W. Ziolkowski, Phys. Rev. E **52**, 5338 (1995).
[19] P. Saari and K. Reivelt, Phys. Rev. Lett. **79**, 4135 (1997).
[20] K. Reivelt and P. Saari, J. Opt. Soc. Am. A **17**, 1785 (2000).
[21] A.P. Kiselev and M.V. Perel, J. Math. Phys. **41**, 1934 (2000).
[22] G.N. Borzdov, in *ESA SP-444 Proceedings of the Millennium Conference on Antennas & Propagation AP2000, Davos, 2000* (ESA, ESTEC, Noordwijk, 2000), pp. 0131 and 0132.
[23] G.N. Borzdov, Phys. Rev. E **61**, 4462 (2000).
[24] G.N. Borzdov, Phys. Rev. E **63**, 036606 (2001).
[25] G. N. Borzdov, in *Proceedings of Bianisotropics 2000: 8th International Conference on Electromagnetics of Complex Media, Lisbon, 2000*, edited by A. M. Barbosa and A. L. Topa (Instituto de Telecomucacões, Lisbon, 2000), pp. 11–14, 55–58, and pp. 59–62.

[26] G.N. Borzdov, AEU Int. J. Electron. Commun. **55**, 224 (2001).
[27] G.N. Borzdov, J. Phys. A **34**, 6249 (2001); **34**, 6259 (2001); **34**, 6269 (2001); **34**, 6281 (2001).
[28] G.N. Borzdov, Proc. SPIE **4467**, 57 (2001).
[29] G.N. Borzdov, Opt. Commun. **94**, 159 (1992); J. Math. Phys. **34**, 3162 (1993).
[30] G.N. Borzdov, in *Electromagnetic Fields in Unconventional Materials and Structures*, edited by O.N. Singh and A. Lakhtakia (Wiley Intersience, New York, 2000), pp. 83–124.
[31] F.I. Fedorov, *Lorentz Group* (Nauka, Moscow, 1979).
[32] L.M. Barkovsky, G.N. Borzdov, and F.I. Fedorov, Zh. Prikl. Spektrosk. **39**, 996 (1983); L.M. Barkovsky and A.N. Furs, J. Phys. A **30**, 4665 (1997); A.N. Furs and L.M. Barkovsky, *ibid.* **31**, 3241 (1998).
[33] L.D. Landau and E.M. Lipshitz, *Field Theory* (Nauka, Moscow, 1973).